

1 **Protein Representations: Encoding Biological Information for Machine Learning in Biocatalysis**

2 David Harding-Larsen ^a, Jonathan Funk ^a, Niklas Gesmar Madsen ^a, Hani Gharabli ^a, Carlos
3 G. Acevedo-Rocha ^a, Stanislav Mazurenko ^{b, c}, Ditte Hededam Welner ^{a, *}

4
5 ^a The Novo Nordisk Center for Biosustainability, Technical University of Denmark, Søtofts
6 Plads, Bygning 220, 2800 Kgs. Lyngby, Denmark

7 ^b Loschmidt Laboratories, Department of Experimental Biology and RECETOX, Faculty of
8 Science, Masaryk University, Kamenice 5, 625 00 Brno, Czech Republic

9 ^c International Clinical Research Center, St. Anne's University Hospital Brno, Pekarska 53,
10 656 91 Brno, Czech Republic

11 * Corresponding author. E-mail address: diwel@biosustain.dtu.dk

12 13 **Abstract**

14 Enzymes offer a more environmentally friendly and low-impact solution to conventional
15 chemistry, but they often require additional engineering for industrial settings, an endeavor
16 that is challenging and laborious. To address this issue, the power of machine learning can be
17 harnessed to produce predictive models that facilitate *in silico* study and engineering of novel
18 enzymatic properties. However, the conversion from the biological domain to the
19 computational realm requires special attention to ensure the training of accurate and precise
20 models. In this review, we examine the critical step of encoding protein information to
21 numeric representations for use in machine learning. We selected the most important
22 approaches for encoding the three distinct biological protein representations — primary
23 sequence, 3D structure, and dynamics — to explore their requirements for employment and
24 inherent biases. Combined representations of proteins and substrates are also introduced as
25 emergent tools in biocatalysis. We propose the division of fixed representations, a collection
26 of rule-based encoding strategies, and learned representations extracted from the latent spaces
27 of large neural networks. To select the most suitable protein representation, we propose two
28 main factors governing this choice. The first one is the model setup, being influenced by the
29 size of the training dataset and the choice of architecture. The second factor is the model
30 objectives, concerning the assayed property, the difference between wild-type models and
31 mutant predictors, and requirements for explainability. This review is aimed at serving as a
32 source of information and guidance for properly representing enzymes in future machine
33 learning models for biocatalysis.

34 35 36 **Keywords**

37 Machine Learning; Biocatalysis; Protein Representations; Enzyme Engineering;
38 Representation Learning; Protein Dynamics, Predictive Models

42 1. Introduction

43

44 In the current time of climate change and increasing resource depletion, enzyme technology
45 has emerged as a more environmentally friendly and potentially low-impact approach to
46 industrial processes traditionally mediated by conventional chemistry (Buller et al., 2023;
47 Hauer, 2020; Radley et al., 2023; Reetz et al., 2024; Sheldon and Woodley, 2018; Wu et al.,
48 2021). Instead of complicated pathways with a plethora of reagents, extreme conditions, and
49 protection groups, enzymes offer a renewable alternative with high selectivity and tunability
50 (Sheldon and Woodley, 2018; Woodley, 2022; Wu et al., 2021). Early examples consist of
51 enzyme-based detergents (Kirk et al., 2002) and the employment of nitrile hydratases to
52 synthesize acrylamide (Yamada and Kobayashi, 1996). Recent advances in bioinformatics
53 strategies have enabled the discovery of enzymes with specialized activity (Buller et al.,
54 2023; Hon et al., 2020; Oberg et al., 2023), as well as the engineering of enzymes towards
55 enhanced activity, substrate specificity, enantioselectivity, and thermostability (Galanie et al.,
56 2020; Qu et al., 2020; Renata et al., 2015). Especially the directed evolution (DE) approach
57 of mimicking Darwinian evolution, which was co-awarded with a Nobel Prize to Frances
58 Arnold (Arnold, 2018, 1998, 1996) has seen significant use for enzyme engineering
59 (Bornscheuer and Pohl, 2001; Cherry et al., 1999; Cherry and Fidantsef, 2003; Giver et al.,
60 1998; Stimple et al., 2020; Turner, 2009; Zhao and Arnold, 1999). Enzymatic biocatalysis
61 has had a profound impact in areas such as pharmaceutical drug discovery (Devine et al.,
62 2018; Savile et al., 2010), the cosmetic industry (Heath et al., 2022; Khan and Rathod, 2015),
63 and waste degradation (Bilal et al., 2019; Mohanan et al., 2020), and multiple enzymatic
64 processes have even been developed sequentially to create biocatalytic cascades (France et
65 al., 2017; Gandomkar et al., 2019; Huffman et al., 2019; Nazor et al., 2021; Santacoloma et
66 al., 2011; Sperl and Sieber, 2018).

67

68 The growing use of enzymes has, nonetheless, revealed several challenges when utilizing
69 them for industrial catalysis purposes because they did not evolve to perform optimally in
70 industrial bioreactors where high stability, selectivity, and activity are important to maximize
71 product yields. Despite improvements in protein engineering, enhancing multiple enzyme
72 properties such as activity and stability simultaneously is still a difficult endeavor (Acevedo-
73 Rocha et al., 2018; Calzadiaz-Ramirez et al., 2020; Stimple et al., 2020; Tokuriki et al.,
74 2012), as well as the prediction and control of substrate specificity and regioselectivity —
75 crucial properties for industrial purposes — are often challenging (Harding-Larsen et al.,
76 2023; M. Yang et al., 2018). In this context, machine learning (ML) algorithms have emerged
77 as powerful tools, capable of modeling complex relationships within protein and enzyme
78 datasets. In biocatalysis, ML has facilitated the study and engineering of proteins and led to
79 novel insights for improving enzymatic processes (Kouba et al., 2023; Markus et al., 2023;
80 Mazurenko et al., 2020; Yang et al., 2019). Notable examples include activity and substrate
81 specificity predictors (Robinson et al., 2020), deep learning (DL) models for the estimation of
82 metabolic enzyme activities (Li et al., 2022) and for functional predictions of enzymes
83 (Gligorijević et al., 2021), models for protein solubility predictions (Yang et al., 2016; Y.
84 Yang et al., 2021), and numerous approaches for predicting protein stability changes upon
85 mutagenesis (Blaabjerg et al., 2023; Folkman et al., 2016; Iqbal et al., 2022; Li et al., 2020;
86 Teng et al., 2010). ML has also enabled a more efficient multiparametric optimization

Abbreviations: BLOSUM, BLOck SUBstitution Matrix; CNN, convolutional neural network; DL, deep learning; EC, enzyme commission; ELBO, evidence lower bound; GFP, green fluorescent protein; GNN, graph neural network; KNN, k-nearest neighbors; MD, molecular dynamics; MLDE, machine learning-assisted directed evolution; MSM, Markov state models; OHE, one-hot encoding; PLM, protein language model; QM/MM, quantum mechanics/molecular mechanics; VAE, variational autoencoder, XAI, explainable AI

87 strategy (Kunka et al., 2023; Ma et al., 2021), facilitated *de novo* enzyme design (Yeh et al.,
88 2023), and prediction of non-additive epistatic effects (Cadet et al., 2018, 2022; Li et al.,
89 2021). Finally, ML has been combined with DE in the aptly termed “machine learning-
90 assisted” directed evolution (MLDE), where it has significantly improved the exploration of
91 the sequence-function landscape in the search for enhanced variants (Bruce J. Wittmann et
92 al., 2021; Wu et al., 2019; Xu et al., 2020; Yang et al., 2024, 2019).

93
94 Traditionally, the focus within ML research has often been to refine the algorithms, whereas
95 data representation is treated as a secondary concern. This viewpoint posits that given
96 sufficient data and computational resources, ML models should inherently discern and
97 leverage the most salient features relevant to the task at hand. However, this view overlooks
98 the challenge of producing such large protein datasets of high quality (*i.e.*, reproducibility)
99 and neglects the critical role of data representation in enhancing or limiting a model’s ability
100 to learn (Bengio et al., 2013; Iuchi et al., 2021). Our work addresses the topic of protein
101 representations as a critical step for uniting biology and data science. In biology, a protein is
102 commonly represented by its primary or tertiary structure through categorical or symbolic
103 information, while ML traditionally requires numeric inputs in the forms of vectors, matrices,
104 and tensors. This poses an exciting task of representing proteins in a manner that is both
105 informative for ML models and reflective of the underlying biological properties.

106
107 Interestingly, the concept of inductive biases introduces a nuanced understanding of how ML
108 models approach learning tasks. Inductive biases refer to the assumptions made by a model
109 about the patterns it expects to find in the data before any data is indeed observed. They
110 guide the learning algorithm towards certain solutions over others, effectively shaping the
111 hypothesis space that the model explores (Baxter, 2000). Selecting the right inductive biases
112 — through the strategic representation of data — can significantly facilitate the learning
113 process, enabling models to learn more efficiently and effectively from fewer examples
114 (Baxter, 2000).

115
116 In the context of biocatalysis, these inductive biases arise either manually or by
117 representation learning, and the choices made during the encoding process strongly affect the
118 information captured in the representations. In this review, we investigate the methodologies
119 for protein representation utilizing the protein sequence, structure, or dynamics. We also
120 analyze the assumptions of the inductive biases that are captured in the different
121 representation techniques. We conclude with a discussion about different factors influencing
122 the choice of protein representation.

123 124 **2. Sequence Representations**

125
126 A simple description of a protein is the one-dimensional sequence representation of the
127 molecular structure using an alphabet of 20 amino acids. This leads to an alphanumeric
128 expression of the biomolecular components to easily differentiate between proteins. While
129 simple, the string of single-letter residue codes contains a vast amount of information, from
130 the physicochemical properties of every amino acid to the evolutionary trace of the protein.
131 Sequences are even intrinsically linked to 3D structures and functional properties, making
132 them a rich source of information critical for protein design. However, the development of
133 ML models for predicting protein functions requires precise feature extraction from those
134 sequences. A spectrum of methodologies to identify optimal features are available, ranging
135 from simple to complex ones. This section outlines the evolution of feature extraction
136 techniques, emphasizing the transition from elementary assumptions to sophisticated models.

137 Finally, we will treat a mixed representation where structural insights are used to influence
 138 the sequence representation.

139

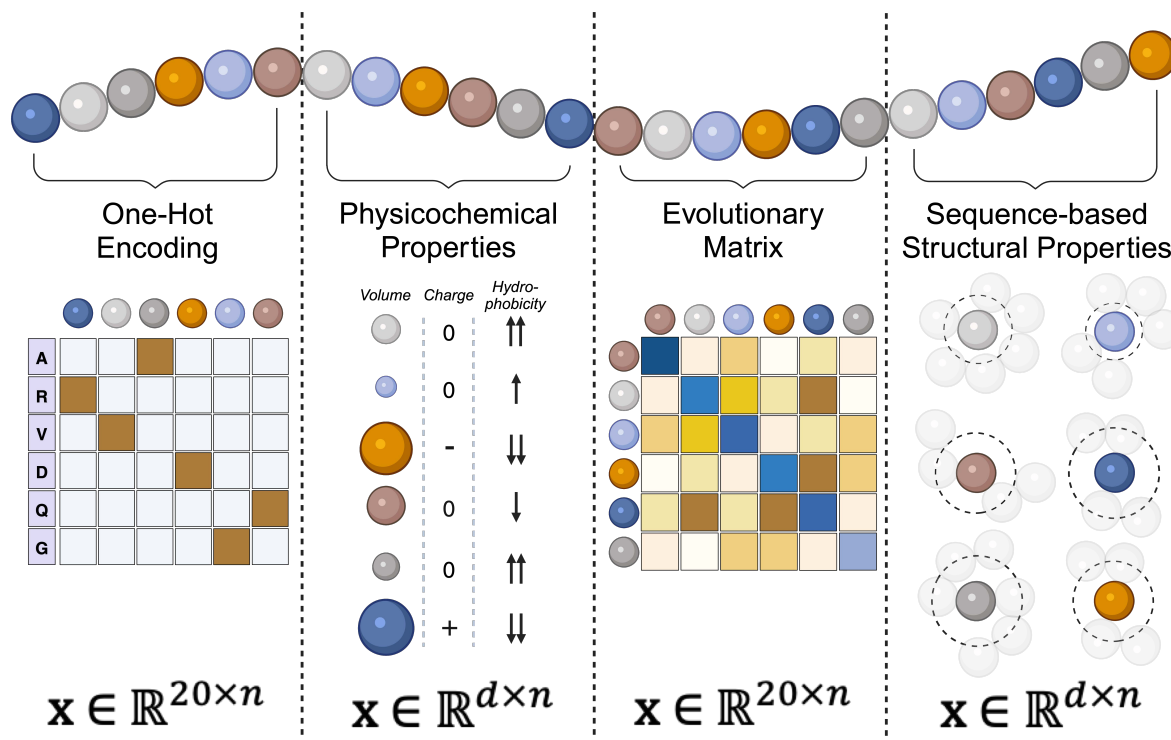
140 2.1 Fixed Sequence Representations

141

142 The methods for capturing biological information stored in the sequence representation are
 143 varied, often focusing on different elements of this information. One category of methods is
 144 the so-called “fixed” representations, a collection of rule-based approaches to convert
 145 between the protein sequence and numerical vectors by incorporating specific parts of the
 146 amino acid characteristics (Figure 1) (Markus et al., 2023). The simplest of all is the one-hot
 147 encoding (OHE) technique, a prevalent method in ML for transforming categorical data into
 148 a binary format. Here, each residue is represented as a vector $v_i = (0, 0, \dots, 1, \dots, 0)$ with ‘1’
 149 placed at the i^{th} index corresponding to its lettering, creating a binary $20 \times N$ matrix with a
 150 single non-zero entry in each column, where N is the length of the protein sequence.

151 Although OHE offers no protein information aside from the amino acid identities, it is used
 152 extensively as a fast and effective method for converting biological information into
 153 numerical vectors (Elabd et al., 2020; Goldman et al., 2022; Greenhalgh et al., 2021; Hsu et
 154 al., 2022; Michael et al., 2023; Raimondi et al., 2019; Bruce J. Wittmann et al., 2021; M.
 155 Yang et al., 2018). However, the sparse and high-dimensional nature of OHE can lead to
 156 computational inefficiencies, particularly in models dealing with long protein sequences.
 157 Moreover, many ML algorithms require the input of a fixed size throughout their training and
 158 inference, necessitating an additional data pre-treatment step in OHE, *e.g.*, trimming long
 159 sequences or extending short ones with zeros.

160



161

162 **Fig. 1. Fixed representations for encoding the protein sequence.** OHE (left) is the simplest method and only
 163 uses the amino acid identity. Physicochemical properties (middle left) instead capture the nature of the amino
 164 acids by explicitly using their properties as features. Matrices such as the BLOSUM encoding introduce
 165 evolutionary information to the protein representation (middle-right). Lastly, the sequence can also be used
 166 to calculate structural properties such as SASA (right).

167 The simple nature and lack of inherent bias prevent OHE from capturing any relationships
168 between amino acids before the training. Property-based encoding strategies emerge as a
169 potential solution to instruct ML algorithms about the physicochemical nature of the
170 sequences, either global protein descriptors or those at the residue level. The former captures
171 the behavior of the entire protein chain through properties such as solubility or radius of
172 gyration, while the latter instead enables the encoding of each amino acid using a set of
173 properties such as charge, hydrophobicity, volume, or pK_a, imposing representation biases
174 towards certain residue attributes and allowing the model to discern the similarities and
175 differences between two residues. Various sets of physicochemical residue descriptors exist,
176 such as the large database of amino acid indices, and AAindex (Kawashima and Kanehisa,
177 2000), containing over 500 matrices for encoding sequence information. Such a set of indices
178 for charge, polarity, hydrophobicity, average accessible surface area, and side chain volume
179 was used to model and predict the donor specificity of fold A glycosyltransferases by Taujale
180 et al. (Taujale et al., 2020). Another example is the recent pre-print by Xu et al., where the
181 authors employ physicochemical properties such as volume, hydrophobicity, and π - π
182 interactions to model and improve enantioselectivity of carboxylesterase AcEst1 from
183 *Acinetobacter sp. JNU9335* (Xu et al., 2024).

184
185 Instead of manually choosing between the many similar indices, the inherent patterns of the
186 physicochemical properties can be extracted through their principle components, such as the
187 Vectors of Hydrophobic, Steric, and Electronic properties (VSHE) (Mei et al., 2005), z-
188 scales (Hellberg et al., 1987; Jonsson et al., 1989; Sandberg et al., 1998; Wold et al., 2011),
189 the DL-based amino acid parameter representations by Meiler et al. (Meiler et al., 2001), or
190 the five factors described by Atchley et al. (Atchley et al., 2005). Using these principal
191 components enables the incorporation of a wide range of different residue properties without
192 drastically increasing the dimensionality of the vector representation due to the principal
193 components containing information from multiple physicochemical properties. An example
194 is Factor III by Atchley et al. which encompasses bulkiness, residue volume, average volume
195 of a buried residue, side chain volume, and molecular weight (Atchley et al., 2005). Several
196 ML models have employed these dimension-reduced physicochemical representations for
197 different enzymes, including the thiolase activity and substrate specificity predictors
198 (Robinson et al., 2020), the Sortase A mutagenesis model for ML-guided directed evolution
199 (Saito et al., 2021), and DeepTM, a DL-based model for predicting the melting temperatures
200 of proteins such as PET plastic-degrading enzymes (M. Li et al., 2023). Nevertheless, a
201 potential issue with this approach is the “black box”-like nature, complicating the process of
202 interpreting the results and discerning the actual residue property contributions when
203 examining model feature importance.

204
205 Aside from introducing residue information and imposing an inherent bias to the protein
206 representation through physicochemical properties, the encoding method can be based on the
207 evolutionary information contained in the sequence. These biases force the model to learn
208 evolutionary important patterns. One such technique, the BLOck SUBstitution Matrix
209 (BLOSUM) encoding, is generated from alignments of protein sequences and focuses on
210 evolutionary changes and conservation (Henikoff and Henikoff, 1992; Mount, 2008). Based
211 on the frequency of amino acid substitutions in these alignments, each entry in a BLOSUM
212 matrix represents the likelihood of substitution between amino acids, calculated based on
213 observed substitutions in protein families. In BLOSUM encoding, each amino acid is
214 replaced by a vector derived from the corresponding row in the BLOSUM matrix, $v_i =$
215 (x_A, x_G, \dots, x_Y) where x_A is the likelihood score that the i^{th} residue is substituted with alanine,
216 thus enabling the representation to capture the evolutionary history and functional similarities

217 between amino acids. We employed this sequence representation in our model for predicting
218 glycosyltransferase activity specificity (GASP), which allowed the model to use the
219 evolutionary information to discern the wide array of different glycosyltransferases (Harding-
220 Larsen et al., 2023). The evolutionary information can also be captured using a Position
221 Specific Scoring Matrix (PSSM), a method that uses a Multiple Sequence Alignment (MSA)
222 of a set of proteins to quantify the likelihood p_{ij} that an amino acid at a specific position j
223 mutates into the i^{th} residue. These matrices can be constructed using a sequence similarity
224 program such as PSI-BLAST (Altschul et al., 1997).

225
226 Finally, a fourth approach to extracting biological information from the protein sequences is
227 to exploit the relationship between the primary sequence and the 3D structure. Secondary
228 structure elements have long been possible to estimate purely through primary sequence (Y.
229 Yang et al., 2018), and also structural properties such as Solvent Accessible Surface Area
230 (SASA) (Lee and Richards, 1971) and the Half Sphere Exposure (HSE) (Hamelryck, 2005)
231 can be predicted from sequence alone (Cheng et al., 2005; Fraczkiewicz and Braun, 1998;
232 Heffernan et al., 2017; Song et al., 2008). Sequence-based structural properties have been
233 used in tandem with metabolic network properties, reaction thermodynamics, and assay
234 conditions to predict WT metabolic enzyme turnover numbers (Heckmann et al., 2020,
235 2018), exhibiting significant importance compared to the other model features. Sequence-
236 based structural properties were also applied in the previously mentioned DeepTM (M. Li et
237 al., 2023) algorithm, again as part of a larger feature set.

238
239 Lastly, it should be noted that the development of AlphaFold2 (Jumper et al., 2021) and
240 similar sequence-to-structure tools (Ahdritz et al., 2022; Baek et al., 2021; Lin et al., 2023)
241 has blurred the boundary between sequence- and structure-based protein representations, as
242 these tools are capable of predicting the entire 3D structure using only the sequence. This
243 ambiguity is necessary to consider, *e.g.*, for fair comparison of sequence-only encoding
244 techniques and algorithms.

245

246 **2.2 Representation learning**

247

248 An alternative to manually extracting features from sequence information is to learn features
249 or representations of sequences through machine learning from data (Iuchi et al., 2021; Sinai
250 and Kelsic, 2020). The key idea is to learn general representations through a machine model
251 by training on large data sets of unlabeled protein sequences. The obtained representations of
252 the pre-trained embedding model are then used to train a task-specific (surrogate) model,
253 requiring less labeled data. The following sections will describe two common approaches for
254 learning sequence embeddings (Figure 2).

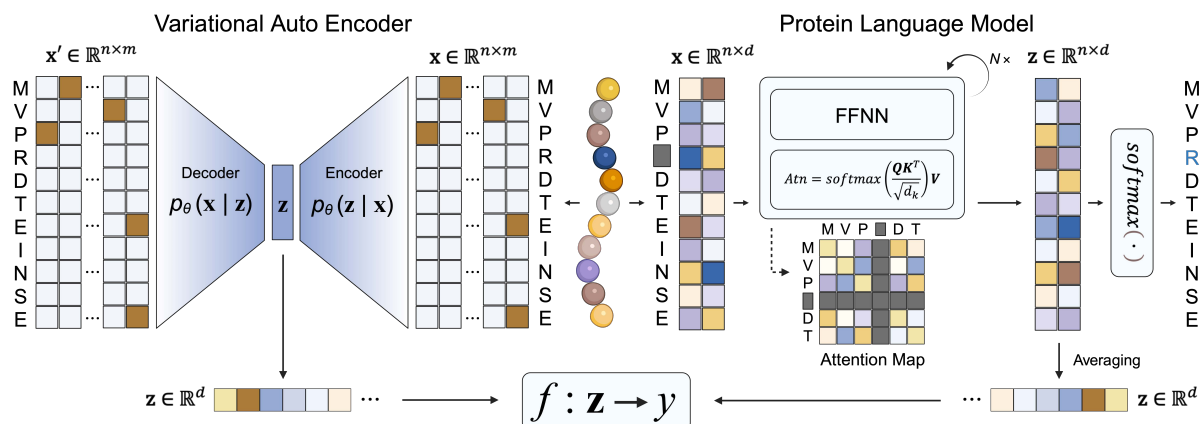
255

256 **2.2.1 Variational Autoencoders**

257

258 Variational Autoencoders (VAEs), introduced by Kingma and Welling in 2013 (Kingma and
259 Welling, 2013), offer a framework for training deep latent variable models that learn
260 meaningful representations by optimizing a lower bound on the likelihood of the data,
261 essentially trying to maximize the probability of observing the training data under the model.
262 This process involves a balance between accurately reconstructing data and enforcing a
263 structured latent space, making it possible for VAEs to generate new data samples that
264 resemble the original inputs. This allows VAEs to capture essential features of the data
265 efficiently. The utility of VAEs is particularly evident in handling high-dimensional and

266 sparse data, such as large sets of one-hot encoded (OHE) protein sequences, enabling the
 267 extraction of compact and meaningful representations (Detlefsen et al., 2022).
 268



269 **Fig. 2. Two common approaches for learning sequence embedding.** Variational Autoencoders (left) are
 270 latent variable models that utilize an encoder-decoder setup to learn a latent space embedding, z . Protein
 271 Language Models (right) are also used to generate sequence representations but instead employ an attention
 272 mechanism that dynamically weighs the relevance of different parts of a protein and a Feedforward Neural
 273 Network (FFNN). A protein encoding can be obtained by averaging over the neural embeddings. The resulting
 274 representations from both techniques can then be used for fine-tuning task-specific predictions.
 275

276
 277 The foundation of VAEs is centered around the transformation of input data (*e.g.* OHE
 278 sequences), x , into a latent distribution, z , through an encoder, $q_\theta(z|x)$. The latent distribution,
 279 typically Gaussian, is characterized by parameters (mean and variance) derived from the
 280 input by a neural network. The decoder of the VAE then attempts to reconstruct the input
 281 data from the latent variables, following the distribution $p_\theta(x|z)$. The objective of training a
 282 VAE is to maximize the evidence lower bound (ELBO) on the log-likelihood, which is
 283 expressed as:

$$284 \mathcal{L}(x; \theta, \phi) = \mathbb{E}_{q_\theta(z|x)} [\log p_\phi(x|z)] - D_{KL}(q_\theta(z|x) || p(z))$$

285
 286 The first term in the ELBO represents the reconstruction loss, promoting similarity between
 287 the decoded samples and the original inputs, and the second term is the Kullback-Leibler
 288 (KL) divergence, serving as a regularization term ensuring that the latent space is well-
 289 regularized and continuous, enabling efficient data representation and interpolation
 290 (Tschannen et al., 2018; Vincent et al., 2008).
 291

292
 293 In the context of protein sequences, VAEs leverage the manifold hypothesis, which suggests
 294 that high-dimensional data can be effectively modeled on a low-dimensional, non-linear
 295 manifold (Vincent et al., 2008). VAEs achieve two critical objectives: (i) reducing the
 296 dimensionality and sparsity to mitigate the curse of high dimensionality (Bellman, 1966) and
 297 (ii) incorporating domain-specific knowledge through the model architecture and sequence
 298 preprocessing and sequence alignment (Detlefsen et al., 2022). Choices made when building
 299 the architecture and constructing the MSA not only facilitate more efficient learning but also
 300 enhance the model's ability to support transfer learning by introducing inductive biases that
 301 align with the tree topology of the evolutionary history underlying the protein family (Ding et
 302 al., 2019). For these among other reasons, latent variable models such as VAEs have seen
 303 widespread adoption for predicting the mutational effect on protein fitness and in MLDE.
 304 Notable examples are the mutational effect predictor EVE by Frazer et al. (Frazer et al.,
 305 2021) or applications in MLDE studies conducted by Wittmann et al. (Bruce J Wittmann et

306 al., 2021; Bruce J. Wittmann et al., 2021). Giessel et al. utilized Variational Autoencoders to
307 engineer therapeutic enzyme variants with improved stability and activity, showcasing the
308 model's ability to generate novel ornithine transcarbamylase sequences with enhanced
309 therapeutic potential, marking a significant advancement in the application of VAEs for
310 therapeutic enzyme engineering (Giessel et al., 2022). Hawkins-Hooker et al. successfully
311 employed Variational Autoencoders to generate novel, functional variants of the luxA
312 bacterial luciferase, demonstrating VAEs' capacity to explore protein sequence space and
313 manipulate biophysical properties such as solubility, thereby presenting a valuable
314 complement to traditional protein engineering methods (Hawkins-Hooker et al., 2021).
315 Kohout et al. leverage VAEs to design novel variants of haloalkane dehalogenases for
316 biocatalysis, demonstrating the applicability to generate sequences with stability and activity
317 comparable to wild types while addressing challenges in maintaining protein solubility
318 (Kohout et al., 2023). Finally, Hsu et al. highlighted the versatility of VAEs by augmenting
319 evolutionary density scores extracted from the DeepSequence VAE model (Riesselman et al.,
320 2018) with the simplistic OHE (Hsu et al., 2022). The augmentation approach achieved high
321 performance across 19 different datasets — even models trained on as few data points as 42.
322

323 2.2.2 Protein Language Models

324
325 Another common method for generating protein sequence representations is Protein
326 Language Models (PLMs), which nowadays increasingly employ the Transformer
327 architecture (Vaswani et al., 2017). The Transformer is an ML architecture originally
328 popularized in the domain of natural language processing to learn general patterns of
329 language by predicting the missing words intentionally removed from sentences by their
330 context. PLMs are trained on large protein sequence databases containing sequences sampled
331 across different organisms. The training objective of PLMs is to reconstruct the sequence of a
332 protein after it has been partially corrupted through the masked language modeling objective
333 (Devlin et al., 2018). Similar to VAEs, PLMs can be used to extract latent representations of
334 protein sequences, by forward passing sequences through the trained model and averaging the
335 final layer output over the sequence length (Rao et al., 2020). A major difference between
336 PLMs and VAEs is the attention mechanism at the core of PLMs, which allows the network
337 to build up complex representations that incorporate context from across sequences (Rives et
338 al., 2021):
339

$$340 \quad \text{Attention}(\mathbf{Q}, \mathbf{K}, \mathbf{V}) = \text{softmax}\left(\frac{\mathbf{Q}\mathbf{K}^T}{\sqrt{d_k}}\right)\mathbf{V}$$

341
342 The attention mechanism used in Protein Language Models (PLMs) dynamically weighs the
343 relevance of different parts of a protein sequence by calculating a weighted sum of values
344 (\mathbf{V}). The weights are determined by the compatibility of queries (\mathbf{Q}) and keys (\mathbf{K}), which is
345 scaled by a constant, the square root of the dimension of the keys (d_k) in the original
346 transformer implementation (Vaswani et al., 2017), and normalized through a softmax
347 function. Analysis of PLM representations has revealed that PLMs intrinsically learn
348 biologically relevant features. For instance, their attention maps have been shown to bear a
349 close resemblance to contact maps in proteins, indicating their capability to capture essential
350 biological insights (Rives et al., 2021). PLM representations have demonstrated great
351 flexibility in domain-specific tasks, such as function prediction, protein localization, and
352 mutational effect prediction (Brandes et al., 2022; Elnaggar et al., 2021; Ferruz et al., 2022;
353 Goldman et al., 2022; Rives et al., 2021; Thumuluri et al., 2022). PLMs offer a robust way to
354 generate highly effective representations for domain-specific applications, making them a

355 popular choice when creating ML models for biocatalysis. Examples of PLMs for
356 biocatalysis include the study by Yu et al. utilizing contrastive learning for the precise
357 annotation of enzyme functions by Enzyme Commission (EC) numbers, outperforming
358 conventional tools in accuracy and capability to annotate underexplored and mislabeled
359 enzymes (Yu et al., 2023). Hoffbauer and Strodel introduce TransMEP, a tool employing
360 transfer learning from protein language models to accurately predict the effects of mutations
361 on proteins, demonstrating the efficacy of leveraging pre-trained models like ESM-2 (Lin et
362 al., 2023) for mutation effect prediction in protein engineering (Hoffbauer and Strodel, 2024).
363 The pre-trained model of ESM-1b (Rives et al., 2021) has also seen extensive use in
364 biocatalysis, either directly employed as protein representations for supervised tasks
365 (Goldman et al., 2022; Hou et al., 2023; Bruce J. Wittmann et al., 2021; Xu et al., 2022), or in
366 the form of a fine-tuned task-specific encodings (Kroll et al., 2023a, 2023b).

367

368 **2.2.3 Comparing VAEs with PLMs**

369

370 Both PLM and VAE representations frequently rank as the state of the art in task-specific
371 application benchmarks, such as mutational effect prediction (Livesey and Marsh, 2023) or
372 MLDE studies (Bruce J. Wittmann et al., 2021). When comparing VAEs to PLMs for
373 applications in protein engineering, some general rules can be drawn. There are some
374 indications that VAEs show greater performance for task-specific applications (Bruce J.
375 Wittmann et al., 2021). VAEs are also smaller than PLMs, which makes them faster at
376 inference and easier to run without large computational resources. Furthermore, VAEs are
377 superior during sampling, due to their ability to easily sample from the latent distribution by
378 passing latent variables through the decoder. VAEs can be highly customized, for example,
379 allowing the creation of latent variables with fewer dimensions to facilitate data visualization
380 or fine-tuning (Detlefsen et al., 2022). On the other hand, VAEs have to be trained
381 individually for each protein family, whereas PLMs can be used across all protein families
382 without further training, even generalizing beyond naturally observed proteins (Verkuil et al.,
383 2022). Interestingly, nowadays ML developers are exploring the possibility of combining
384 PLMs and VAEs (Sevgen et al., 2023).

385

386 **2.3 Structure-Informed Sequence Representations**

387

388 Some methods incorporate structural information when producing a sequence representation.
389 Here, the protein structure is employed as a selection filter for the identification of important
390 residues, delimiting the sequence encoding to a curated list of amino acids and circumventing
391 the issue of information dilution where redundant features dominate the informative ones. For
392 biocatalysis, these structure-informed sequence representations ensure that the focus is
393 directed towards important parts of the enzyme, such as the active site, remote binding sites,
394 or other areas believed to be important for the enzymatic property to be modeled (*e.g.*, dimer
395 interfaces).

396

397 In structure-informed sequence representations, a 3D structure is combined with an MSA to
398 identify and encode specific residues in every protein of interest. Generally, two different
399 approaches exist for this identification: manual selection and spherical extraction. The former
400 method entails examining the template structure and choosing the residues important for the
401 area in focus such as the residues lining the active site as described by Röttig et al. in their
402 Active Site Classification (ASC) strategy to model the protein families of kinases, nucleotidyl
403 cyclases, trypsins, malate/lactate dehydrogenases, and decarboxylating dehydrogenases
404 (Röttig et al., 2010). The list of manually curated residues is then mapped onto every protein

405 in the MSA through the aligned positions of the identified residues. In the spherical
406 extraction method, the list of important residues is instead acquired automatically by
407 constructing a spherical boundary around the area in focus, *e.g.*, the catalytic residues, and
408 then extracting all amino acids encompassed by this boundary using protein structure analysis
409 programs such as MDTraj (McGibbon et al., 2015) or BioPython (Cock et al., 2009). This
410 automated selection approach was employed by Robinson et al. to model and predict the
411 substrate specificity of OleA thiolases; aligning all 73 sequences to the OleA thiolase from
412 *Xanthomonas campestris* (Goblirsch et al., 2016) and extracting the active site residues from
413 a crystal structure of the before-mentioned protein using a 12 Å sphere centered around the
414 C_α of the active site cysteine (Robinson et al., 2020). Another example is Goldman et al. who
415 examined the activity and substrate specificity of multiple protein families including
416 glycosyltransferases and halogenases using spheres ranging from 3 to 30 Å (Goldman et al.,
417 2022).

418
419 Both selection strategies have their merits and deficiencies: while manual selection ensures a
420 significant degree of control over the choice of residues, it ultimately requires expert curation
421 and is highly protein-specific. The spherical extraction technique sacrifices some of this
422 control to alleviate these issues by only needing the centroid and radius to be defined, making
423 the process faster than the manual selection.

424
425 Importantly, the structure-informed approach currently requires an MSA to map the identified
426 residues to the entire set of proteins, which might cause problems for poor alignments with
427 many gaps that offer minimal protein information. Furthermore, while the strategy can be
428 used to bias the representation to focus on specific areas of the protein, discarding a
429 significant portion of the sequence is also an inherent limitation of the method. If a distant
430 part of the protein is important for a property, *e.g.*, due to allostery influencing protein
431 activity (Calvó-Tusell et al., 2022a), this information will be lost when only focusing on a
432 specific site. Furthermore, if an ML model targets global properties such as protein fitness
433 scores (Fox, 2005; Michael et al., 2023; Bruce J. Wittmann et al., 2021; Wu et al., 2019) or
434 melting temperature (M. Li et al., 2023), it is unlikely to benefit from focusing the protein
435 representation on a particular part of the protein.

436 437 **3. Structure Representations**

438
439 The biological structure representation contains information about the relative 3D positions
440 and chemical identities of every atom and bond of the protein, $\mathbf{x} = \mathbb{R}^{3 \times N}$, with N being the
441 length of the sequence. Increasing the information complexity from a 1D amino acid
442 sequence to a 3D structure thus introduces additional challenges for the encoding, especially
443 when working with simpler ML architectures requiring an abstraction of the protein structure
444 into a one-dimensional representation vector. Encoding the protein structure can either be
445 done by extracting fixed features directly from the structure or by converting the highly
446 detailed 3D protein into a simpler representation for producing learned representations.
447 Alternatively, it can be done by utilizing a novel structure alphabet.

448 449 **3.1 Fixed Features Extracted from the Protein Structure**

450
451 Similar to describing the sequence through a set of fixed properties, fixed structure
452 representations can be constructed by quantifying different aspects of the protein structure.
453 While the use of these structural features has been limited in ML for biocatalysis, several
454 approaches exist for extracting features from the 3D structure of a protein. Many enzymes

455 utilize a binding pocket to tailor the catalytic environment, which can be converted to
456 numerical descriptors through tools such as Fpocket (Le Guilloux et al., 2009), a program for
457 detecting and describing ligand-binding pockets. Features from Fpocket have seen use in
458 allosteric site prediction (Xiao et al., 2022). Accurate van der Waals surface area descriptors,
459 moments of inertia, electrostatics, and thermodynamic values can be calculated through
460 programs such as ProtD-Cal (Ruiz-Blanco et al., 2015), and those features have seen use in
461 models predicting the substrate specificity of nitrilases (Mou et al., 2021) or estimating the
462 kinetic parameters of glycoside hydrolases (Carlin et al., 2016).

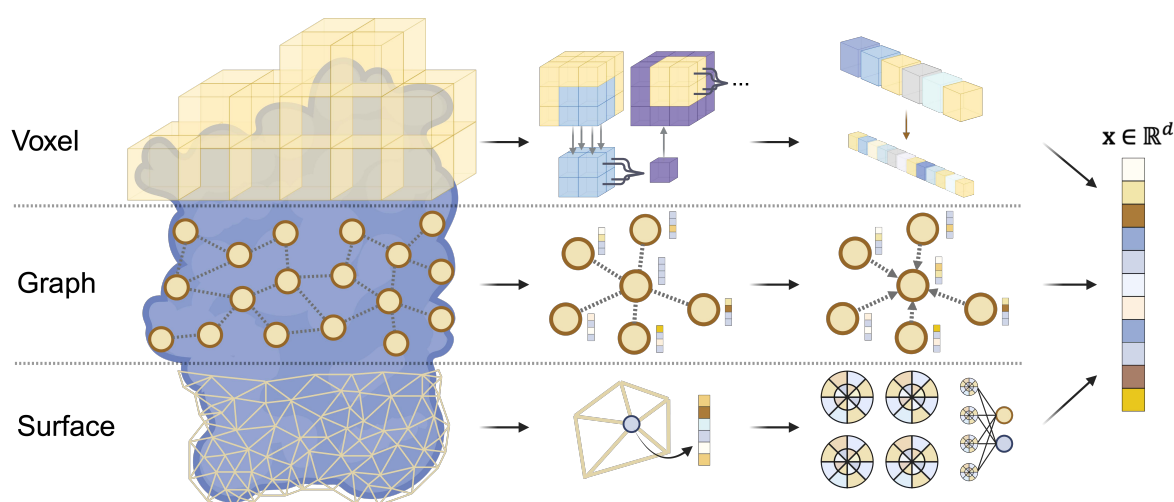
463

464 3.2 Simplification of the 3D Protein Structure for Representation Learning

465

466 Instead of distilling the structural information into a set of descriptors, the structural data can
467 be converted into simplified representations that retain more information than fixed structure
468 features. This can be done with a cubic grid (voxel), protein graph representations, or protein
469 surface representations. These methods can then be employed in DL architectures to
470 construct learned protein representations (Figure 3) (Isert et al., 2023).

471



472

473 **Fig. 3. Three common structure representations for DL architectures and their process towards a learned**

474 **1D vector representation $\mathbf{x} \in \mathbb{R}^d$.** Top: the protein structure is approximated using a 3D voxel grid
475 representation. This grid is processed using a 3D CNN, where voxels are sequentially convoluted to reach the
476 desired dimensions. Middle: the protein graph is a non-linear representation of the structure using nodes and
477 edges. In the GNN, the properties of each node are passed through the edges to update the node information.
478 Bottom: Triangulation creates a protein surface representation with each vertex containing physicochemical
479 information. The mesh is usually deformed to a polar coordinate system and processed using a convolutional
480 network.

481

482 3.2.1 Grid Representations

483

484 The continuous protein structure can be converted to a discrete representation by dividing the
485 molecular space into individual grid sections. Volumetric cubes — so-called voxels —
486 represent 3D data by an assembly of course-grained cubes, drastically reducing the
487 dimensions of the encoding (Isert et al., 2023). This can either be implemented by dividing
488 the structure into smaller “microenvironments” and then encoding each of these
489 microenvironments individually (Paik et al., 2023; Shroff et al., 2020; Torng and Altman,
490 2017), or by encoding the entire protein into a single arrangement of cubes based on a regular
491 3D grid (Amidi et al., 2018).

492

493 MutCompute is a tool that utilizes the former strategy of microenvironments (Paik et al.,
494 2023; Shroff et al., 2020). For every residue in each protein, a cubic 20Å microenvironment
495 is represented by 1Å voxel cubes containing information about atom labels, partial charges,
496 and solvent accessibility of each atom within the voxel cube. The microenvironment
497 representation is then processed by a 3D convolutional neural network (CNN) and later a
498 fully connected neural network (FCNN). This allows the authors to evaluate the chemical and
499 steric suitability of each of the 20 natural amino acids. This can be used as the basis for
500 mutagenesis, such as highlighted by the study achieving an improved thermostability of the
501 *Bacillus stearothermophilus* DNA polymerase (Paik et al., 2023). Novel work has expanded
502 upon the model of MutCompute, introducing information about phosphorus and grouped
503 halogens and thereby facilitating the training on heterogeneous microenvironments
504 (d’Oelsnitz et al., 2024). The new model, MutComputeX, was employed for the engineering
505 of activity-enriched variants of methyltransferase.

506
507 Instead of dividing the protein structure into smaller segments, Amidi et al. employed the
508 entire protein structure in their encoding strategy (Amidi et al., 2018). The protein backbone
509 is converted into a binary voxel grid with a predefined resolution and processed by a 3D
510 CNN. The model was trained to predict EC numbers, achieving an accuracy of 78.4%. The
511 authors furthermore highlighted the versatility of this approach, as the model’s binary voxel
512 representation can be replaced by physicochemical properties such as hydrophobicity and
513 isoelectric points. This allows future models to include inductive biases tailor-made for a
514 specific task. It should be noted that while the voxel representation can directly capture the
515 3D nature of proteins, it is not without limitations. For example, it is sensitive to rotations and
516 translations of a 3D structure in space and does not directly capture information about
517 chemical bonds.

518 519 **3.2.2 Protein Graphs**

520
521 An alternative approach to grid representations is to collapse the 3D protein structure to a
522 graph representation where the structural information of the protein is encoded as elements
523 and connections, designated as “vertices”/“nodes” and “edges”, respectively (Fasoulis et al.,
524 2021). Different detail levels can be employed when creating protein graphs, *e.g.*, for
525 atomistic resolution, features of each node consist of atom type and charge, while the edges
526 represent the molecular bonds (Fasoulis et al., 2021). A more coarse-grained approach is the
527 residue-level description where the nodes represent entire amino acids and the edges specify
528 both the covalent and non-covalent interactions between the residues. For residue-level
529 protein graphs, the node features can include physicochemical properties such as polarity and
530 hydrophobicity (Fasoulis et al., 2021), or more advanced residue encodings such as
531 evolutionary information or secondary structure (M. Li et al., 2023). Importantly, a graph is a
532 non-linear data structure. The node connections can be represented using adjacency matrices
533 where the i^{th} element in the j^{th} row describes the edge between the i^{th} and the j^{th} node, with the
534 ordering of the nodes being arbitrary. The protein contact map is an example of an adjacency
535 matrix.

536
537 Due to the non-linearity of graph representations, it is often infeasible to combine them with a
538 classical ML architecture, such as logistic regression or tree-based models. This processing
539 issue is solved by employing Graph Neural Networks (GNNs), a network architecture that
540 directly implements the graph representation in model construction. In contrast to traditional
541 neural networks where the information is passed through a series of hidden layers, GNNs
542 utilize the edges as channels for information transfer between the individual nodes. This

543 ensures that only information originating from neighboring nodes within a pre-defined
544 proximity is used to update each node (Zhou et al., 2020).

545
546 An exciting example of a GNN-based enzyme predictor is DeepFRI, a model leveraging both
547 sequence and structure representations to model Gene Ontology (GO) terms and EC numbers
548 (Gligorijević et al., 2021). Here, the sequence embeddings of a pre-trained PLM are used as
549 residue nodes while a protein contact map is utilized as graph edges. A recent pre-print also
550 proposed to combine the ESM2 sequence embeddings with graph-based structure
551 embeddings for downstream tasks, such as predicting EC numbers, introducing the Protein
552 Structure Transformer (PST) architecture, outperforming previous state-of-the-art models
553 (Chen et al., 2024).

554
555 It should be noted that while building GNNs requires a significant amount of data, pre-trained
556 structure embeddings can be utilized as protein encodings, drawing a parallel to the pre-
557 trained sequence embeddings. This was highlighted by the authors of PST, exhibiting high
558 performance using pre-trained protein embeddings extracted from the model (Chen et al.,
559 2024). Another example is the Masked Inverse Folding (MIF) model (K. K. Yang et al.,
560 2022), a GNN trained on the sequences and structures of 19,000 proteins in the CATH4.2
561 dataset (Dawson et al., 2019, 2017) to reconstruct a corrupted protein sequence using
562 backbone information. The MIF embeddings have seen use as a representation of the protein
563 structure (Hou et al., 2023), where the power of GNNs is harnessed to process structural
564 information without requiring either a large dataset or computationally costly model training.

565 566 **3.2.3 Surface Encodings**

567
568 Finally, the protein can be modeled using a mesh-based variant of the molecular surface, a
569 continuous sheet describing the accessibility trace of the molecule using a probe of a given
570 radius (Richards, 1977). An example is the surface used for calculating the previously
571 mentioned SASA, where the contact surface is the parts of the atomic van der Waals spheres
572 in contact with the probe. The continuous surface can be discretized using triangulation,
573 where the curvature is converted into a protein polygon mesh using tools such as MSMS
574 (Sanner et al., 1996). These surface meshes are often encoded with the physicochemical
575 information of the residues or atoms, allowing them to function as protein representations in
576 ML models.

577
578 Notable examples of models harnessing surface representations include molecular surface
579 interaction fingerprinting MaSIF (Gainza et al., 2019). In this example, the surface is here
580 segmented by assigning radial patches to every vertex in the protein mesh and generating an
581 overlapping collection of surface vertices. Geometric features and chemical properties are
582 calculated for each vertex within the patches, and the mesh is mapped to a polar coordinate
583 system. This representation is passed through a convolutional architecture that produces
584 learned fingerprint descriptors. The authors utilized these fingerprints to classify ligand-
585 binding pockets, predict protein-protein interaction sites, and estimate the structural
586 configurations of protein-protein complexes. While not inherently targeting biocatalysis,
587 Gainza et al. consequentially highlight the advantage of surface presentation learning for
588 understanding protein interactions.

589
590 In SURFMAP, the reduced surface generated by the MSMS tool (Sanner et al., 1996) is
591 employed to generate a set of particles, each 3Å away from the protein surface (Schweke et
592 al., 2022). After mapping the particles with a feature such as hydrophobicity or stickiness

593 related to the closest residue, their spherical coordinates are projected onto a 2D map using
594 the Sanson-Flamsteed 2D projection. The authors employed this simplified representation to
595 construct a hierarchical clustering model of superoxidase dismutases. This allowed them to
596 distinguish between enzymes with different oligomerization states and metal ion binding
597 preferences. Lastly, the HoloProt model combined structure- and surface-based graphs in
598 multi-scale graph representation to predict enzyme classifications and protein-ligand binding
599 affinities (Somnath et al., 2021).

600

601 **3.3 Alternative Structure Representations**

602

603 While we have generally categorized protein structure representation as either fixed
604 descriptors or geometrical simplifications for learned representations, some approaches fall
605 outside of this division. Recently, a novel technique for representing the protein structure
606 using a string of letters has emerged in Foldseek (van Kempen et al., 2023). Originally
607 designed as a tool to efficiently align a query structure against large databases, Kempen et al.
608 developed an intriguing structure encoding. An artificial alphabet — denoted 3Di —
609 describing the tertiary interactions of the protein is generated using a VAE. Each protein is
610 encoded using this 3Di alphabet, and the resulting sequences are parsed through the prefilter
611 modules of MMseqs2 (Steinegger and Söding, 2017), a protein sequence searching tool, to
612 use in alignment queries. The Foldseek structure-to-sequence approach facilitates the use of
613 traditional sequence representation architecture to process structural information (Heinzinger
614 et al., 2023; Sledzieski et al., 2023; Su et al., 2023; Waksman et al., 2024). While no enzyme
615 models have been trained using these 3Di representations as of the writing of this review, we
616 envision this to be an exciting area for future utilization of structural information.

617

618 **4. Dynamics Representation**

619

620 At the heart of enzymology lies the dynamic nature of enzymes (Henzler-Wildman and Kern,
621 2007), a realm where static structural protein models meet their limits (Lane, 2023). Enzyme
622 dynamics are becoming a key ingredient to understanding and engineering enzyme function,
623 yet the incorporation of dynamic representations in ML remains in its infancy. Enzyme
624 dynamics is observed as the collective movements at time scales of femtosecond bond
625 vibrations, nanosecond side-chain fluctuations, and millisecond domain motions. Together,
626 these motions are termed conformational dynamics and are critical for understanding
627 enzymes (Agarwal et al., 2020; Corbella et al., 2023; Henzler-Wildman and Kern, 2007).

628

629 **4.1 Dynamics as a Tool to Understand, Predict, and Engineer Enzymatic Activity**

630

631 Dynamics are important and offer explanations to why distal mutations accumulate during
632 directed evolution campaigns (Osuna, 2021), why conformational changes such as lid
633 opening/closing rates can be rate-limiting (Wolf-Watz et al., 2004), and how conformational
634 heterogeneity is linked with evolvability of enzyme function (Campbell et al., 2016, 2018;
635 Corbella et al., 2023; Kim and Porter, 2021). Enzyme dynamics form a foundation on which
636 enzymes have been studied rationally, ranging from the canonical β -lactamase (Galdadas et
637 al., 2021), to halogenases (Ainsley et al., 2018), transferases (Tian et al., 2024), lipases
638 (Behera and Balasubramanian, 2023), luciferases (Schenkmyerova et al., 2021),
639 dehalogenases (Vasina et al., 2022), and dehydrogenases (Acevedo-Rocha et al., 2021;
640 Calzadiaz-Ramirez et al., 2020). Dynamics often explain the evolution of enzymes, as they
641 seemingly evolve dynamic networks and freeze out unproductive motions to increase
642 catalytic activity (Bunzel et al., 2021; Campbell et al., 2016).

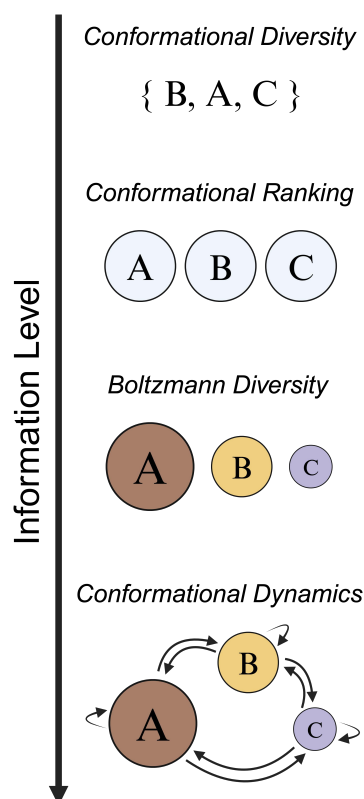
643
644 Predictions of mutant effects on dynamics using statistical tools and algorithms are currently
645 enabling the challenging task of conformationally driven enzyme design (Osuna, 2021). The
646 approaches are, however, not limited to computational tools. Experimentally driven design of
647 dynamics is also underway, enabled by advances in NMR, room-temperature and time-
648 resolved X-ray crystallography, facilitating experimental studies of enzyme dynamics and
649 elucidating its link to activity (Bhattacharya et al., 2022; Broom et al., 2020; Weinert et al.,
650 2017).

651
652 What remains are ML/DL-driven end-to-end solutions for predicting changes in catalytic
653 activity based on dynamic representations. This necessarily requires numerical
654 representations that are well-suited for available architectures. The next frontier of
655 computational biology is to predict the correlation between conformational dynamics and
656 specific mutations, and their effect on activity, work which is well underway. This includes
657 recent works on multi-state design, including simple dynamic representations to predict
658 changes in activity, and ensemble-based enzyme design (Broom et al., 2020; Elia Venanzi et
659 al., 2024; St-Jacques et al., 2023).

660 **4.2 A Primer on Conformational Dynamics**

661
662 Utilizing the temporal dimension of structural biology implies moving from a single structure
663 parameterized computationally by Euclidean coordinates $\mathbf{x} \in \mathbb{R}^{3n}$ to a set of structures $\mathbf{X} =$
664 $\{\mathbf{x}_1, \mathbf{x}_2, \dots, \mathbf{x}_n\}$. The temporal perspective ($\mathbb{R}_{x,y,z}^{3n} \times \mathbb{R}^t$) is challenging for biologists and
665 computational scientists alike, as relevant collective movements must be extracted and
666 correlated with enzymatic properties. It is a significant challenge for both communities to
667 represent these movements efficiently. The task of dynamic representations is thus finding a
668 map between the high-dimensional input using a collection of structures \mathbf{X} to a lower-
669 dimensional representation $f: \mathbf{X} \rightarrow \mathbb{R}^m$, without losing essential information.

670
671 Reflecting contemporary opinions (Vani et al., 2023), it is pertinent to clarify the dynamics of
672 enzymes, which can be defined as a hierarchy of information (Figure 4). While the simplest
673 protein dynamics examination is short-timescale sampling around one conformational state,
674 for systems populated by multiple conformational states, *e.g.*, A, B, and C, conformational
675 diversity is defined as all accessible conformations without any order $\{C, A, B\}$.
676 Conformational ranking implies that the order of relative population is known $\{A, B, C\}$.
677 Boltzmann diversity orders all conformational states with correct Boltzmann weights (relative
678 populations). Lastly, conformational dynamics are all accessible conformational states with
679 correct Boltzmann weights and inter-conversion timescales (arrows in Figure 4). Using these
680 definitions, many approaches do not rigorously describe conformational dynamics, but only
681 aspects on low rungs of the information hierarchy.
682



683
684 **Fig. 4. The hierarchy of information for dynamics.** Conformational Diversity is all accessible conformations
685 without any order, while the order of the relative population is known in Conformational Ranking. Boltzmann
686 Diversity orders all conformational states according to their Boltzmann weights. Lastly, Conformational
687 Dynamics contains all accessible conformational states with correct Boltzmann weights and inter-conversion
688 timescales (arrows).

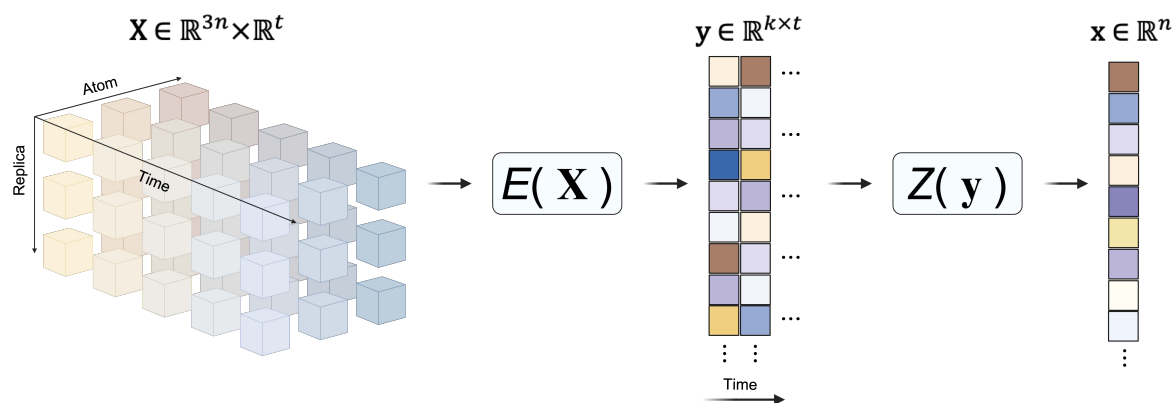
689 4.3 Dimensionality Reduction of MD Simulations

690 Enzyme dynamics is typically studied computationally using long-duration molecular
691 dynamics (MD) simulations *in silico*, based on Newtonian dynamics using small time steps to
692 propagate a system forward a small unit in time (typically femtoseconds, 10^{-15} s). Often, this
693 is carried out for millions of time steps resulting in a high-dimensional representation, and the
694 challenge then lies in reducing dimensionality while conserving relevant dynamics
695 information (Figure 5). These reductions are termed collective variables (Bhakat, 2022).

696 Collective variables were conventionally geometric measures between key catalytic residues
697 and the ligand (Bhakat, 2022). These may represent the temporal fluctuation of distances,
698 angles, or dihedral angles, thus summarising key interactions. The measures are selected
699 based on domain knowledge of enzyme function and mechanism and have been successfully
700 used to predict and engineer enzymes (A.Maria-Solano et al., 2018; Elia Venanzi et al.,
701 2024).

702 Modern collective variables are learned, finding a collective coordinate system that retains
703 crucial information of the dynamic system. Briefly, a linear/non-linear map (E) is estimated
704 which projects the high-dimensional data \mathbf{X} to a lower dimensional space $y = E(\mathbf{X})$ (See
705 Figure 5) (Noé et al., 2020). Common examples include principal component analysis (PCA),
706 and time-lagged independent component analysis (tICA) (Bhakat, 2022; Schultze and
707 Grubmüller, 2021), or a more advanced variational approach for Markov processes
708
709
710
711

712 (VAMPnets) (Ghorbani et al., 2022; Mardt et al., 2018), These are frequently used to
 713 represent the dynamic enzyme system and can help with visualizing the relative population of
 714 conformational states (Acevedo-Rocha et al., 2021; Agarwal et al., 2020; Curado-Carballada
 715 et al., 2019; Romero-Rivera et al., 2017).
 716



717
 718 **Fig. 5. Procuring protein representations from dynamics.** Dynamics are often studied using high
 719 dimensional MD simulations, with \mathbf{X} containing both multidimensional spatial and temporal information. Using
 720 a map, E , lower-dimensional collective variables that summarise the relevant dynamics of the system can be
 721 extracted. The dimensions can be further reduced by averaging over the temporal dimension, $Z(\mathbf{y})$, obtaining
 722 time-averaged variables.
 723

724 In analogy with collective variables, many dynamic representations often remain a function
 725 of time, and time-averaged measures are thus beneficial to further reduce the dimensionality
 726 ($Z(\mathbf{y})$ in Figure 5). For example, root-mean-square deviation (RMSD, $\mathbb{R}^n(t)$) is a time-
 727 dependent measure, but root-mean-square fluctuation (RMSF, \mathbb{R}^n) is not. Time-averaged
 728 measures are popular as they can reduce geometric collective variables (*e.g.* distance
 729 fluctuations) to a single scalar value. While this summarises the entire time series, it is
 730 inherently coarse-grained, thus potentially losing the representation of key dynamic behavior.
 731 Nevertheless, the time-dependent and independent measures (RMSD and RMSF,
 732 respectively) and their variance remain key representations of rigid and mobile regions in
 733 enzymes as well as or indicators of whether catalytically conducive conformations are
 734 sampled. These features can be thought of in the context of the aforementioned map f , in this
 735 case, $Z(E(\mathbf{X}))$, which produces a low-dimensional representation \mathbb{R}^n by summarising the
 736 variability of a collection of structures \mathbf{X} across a simulation (Ainsley et al., 2018;
 737 Audagnotto et al., 2022; Kamerlin and Warshel, 2010).
 738

739 4.4 Multi-state Design

740
 741 Another state-of-the-art strategy is to employ energy-centric methods. These methods cannot
 742 explain anything past the Boltzmann diversity on the conformational information hierarchy
 743 and assume that hinge motions or other major conformational states can be slightly perturbed
 744 in their stability by mutation to favor a desired conformation. These major conformational
 745 states may be contributing to substrate specificity and activity, thus a multi-state design
 746 accounts for the relevant $\Delta\Delta G$ of mutations with respect to the change in conformation (St-
 747 Jacques et al., 2023). This energy-centric representation associates an energy value with each
 748 mutant and conformational state, which may be used to assess the relative stability of
 749 conformational states. In terms of f , each structure \mathbf{x} is assigned an energy which drastically
 750 reduces the dimensionality of the representation.
 751

752 4.5 Shortest Path Map; A Dynamic Representation

753
754 At equilibrium, a more informative representation of dynamics may instead be derived from
755 long-duration MD simulations. These representations elucidate allosteric networks
756 (communication paths between distal residues and the active site) and can be obtained by
757 considering the dynamic cross-correlation matrix made of elements
758

759

$$C_{ij} = \frac{\langle \Delta r_i \cdot \Delta r_j \rangle}{\sqrt{\langle r_i^2 \rangle \langle r_j^2 \rangle}}$$

760 where C_{ij} is the dynamic cross-correlation between residue i and j , $\langle \Delta r_i \cdot \Delta r_j \rangle$ is the time-
761 averaged displacement from the mean coordinate of residue i and j , and $\sqrt{\langle r_i^2 \rangle \langle r_j^2 \rangle}$ is a
762 normalization factor. This representation was developed by the group of Silvia Osuna and
763 recently deployed as a web server (Casadevall et al., 2024), conferring accessibility of
764 dynamic representations. The measure lies one rank above residue-independent measures
765 such as RMSF, as it treats pairs of residues in a dynamic, but time-averaged, context (Morra
766 et al., 2012). One obtains a representation of $\mathbb{R}^{n \times n}$, where n is the number of atoms, a square
767 matrix with information about the covariance of residues. The allosteric networks derived
768 from this representation have been strongly correlated with distal mutations and subsequent
769 effects on catalytic activity. In fact, many directed evolution campaigns accumulate
770 mutations along allosteric networks in retro-aldolase, tryptophan synthase, cytochrome P450
771 oxygenase, imidazole glycerol phosphate synthase, and protein tyrosine phosphatase
772 (Acevedo-Rocha et al., 2021; Calvó-Tusell et al., 2022b; Crean et al., 2021; Gergel et al.,
773 2023; Maria-Solano et al., 2021; Romero-Rivera et al., 2022, 2017). Alternatively,
774 asymmetric measures have also become prevalent, describing the directionality in coupling
775 and thus elucidating residues controlling dynamics (Kazan et al., 2023).
776

777 During catalytic transformation, non-equilibrium dynamics have been observed using
778 advanced MD tools. This so-called D-NEMD method is an alternative but complimentary
779 way of representing allosteric networks from which one obtains a time-dependent vector,
780 $R^n(t)$, that carries information about communication pathways in the catalytic cycle (Castelli
781 et al., 2024; Oliveira et al., 2021).
782

783 **4.6 Learned Dynamic Representations and Future Directions**

784

785 Finally, to address conformational transitions using a full description of conformational
786 dynamics, Markov state models (MSM) are critical as they capture both relative populations
787 and inter-conversion timescales between conformational states (Chodera and Noé, 2014).
788 Despite their initial challenges (Konovalov et al., 2021), MSMs have successfully been
789 applied to explain the dynamic behavior of many enzymes, *e.g.*, polymerases, isomerase,
790 glycosylases, and synthase (Gordon et al., 2016; Konovalov et al., 2021; Wapeesittipan et al.,
791 2019). With subsequent advances in ML, the collective variables are learned and extracted to
792 form a thermodynamic and kinetic basis for understanding the enzyme in question (Ghorbani
793 et al., 2022; Mardt et al., 2018). They are typically represented by a transition probability
794 matrix ($\mathbb{R}^{S \times S}$ where S is the number of discrete states) and a stationary distribution ($\pi =$
795 $[\pi_1, \dots, \pi_S]$) describing the relative population of states, which are obtained from long-duration
796 MDs.
797

798 The representations above are often derived from long-duration MD simulations, and thus
799 limit the use of dynamics data in ML due to their computational cost. This tension lies in the
800 discrepancy between the femtosecond time step of MDs and the microsecond-millisecond

801 timescales at which large conformational changes occur that are important for enzymatic
802 catalysis.

803

804 In principle, however, MD is not the only approach for obtaining a collection of structures X .
805 The field is currently addressing this through the use of ML tools and DL generative models,
806 where X is considered as being derived from a probability distribution $p(x)$. Generating X is
807 thus a question of sampling from $p(x)$. It has been shown that AlphaFold2 can be used to
808 obtain various conformational states of proteins by feeding shallow MSAs (Casadevall et al.,
809 2023; Sala et al., 2023; Wayment-Steele et al., 2024). These methods only obtain
810 conformational diversity on the information hierarchy but have subsequently been extended
811 toward Boltzmann diversity using seeded MD simulations (Audagnotto et al., 2022; Vani et
812 al., 2023). Alternatively, a combination of AlphaFold2 and generative models has also been
813 developed to enable the generation of conformational ensembles (Jing et al., 2024). Thus, a
814 rapidly expanding toolkit with which conformational ensembles can be generated is being
815 established (Arts et al., 2023; Bose et al., 2023; Mansoor et al., 2023; Noé et al., 2020),
816 enabling dynamic representations to be used for in biocatalysis.

817

818 **5. Protein-Substrate Representations**

819

820 In previous sections, the emphasis has been on the featurisation of the protein. However,
821 those strategies do not consider the possible interactions with the protein environments, *e.g.*,
822 solvents, ligands, substrates, or cofactors. This is an integral part of biocatalysis and
823 constitutes a treasure trove of information that could prove beneficial in the training of ML
824 models. The inclusion of protein-substrate interactions would, in most cases, include
825 molecular docking, but could also involve protein dynamics, QM/MM simulations, or even
826 crystallized complexes (Bonk et al., 2019). This could, in turn, assist in addressing tasks such
827 as predicting substrate specificity or elucidating the structure-function of enzymes (Berselli et
828 al., 2021). Within the realm of ML, features extracted from substrate-docking have yet to be
829 fully leveraged (Ao et al., 2024) and are possibly challenged by difficulties in translating
830 protein-substrate complexes into a numerical and general representation. However, some
831 studies have successfully included information harvested from protein-substrate complexes
832 for ML models employing different strategies which will be introduced in this section (Figure
833 6).

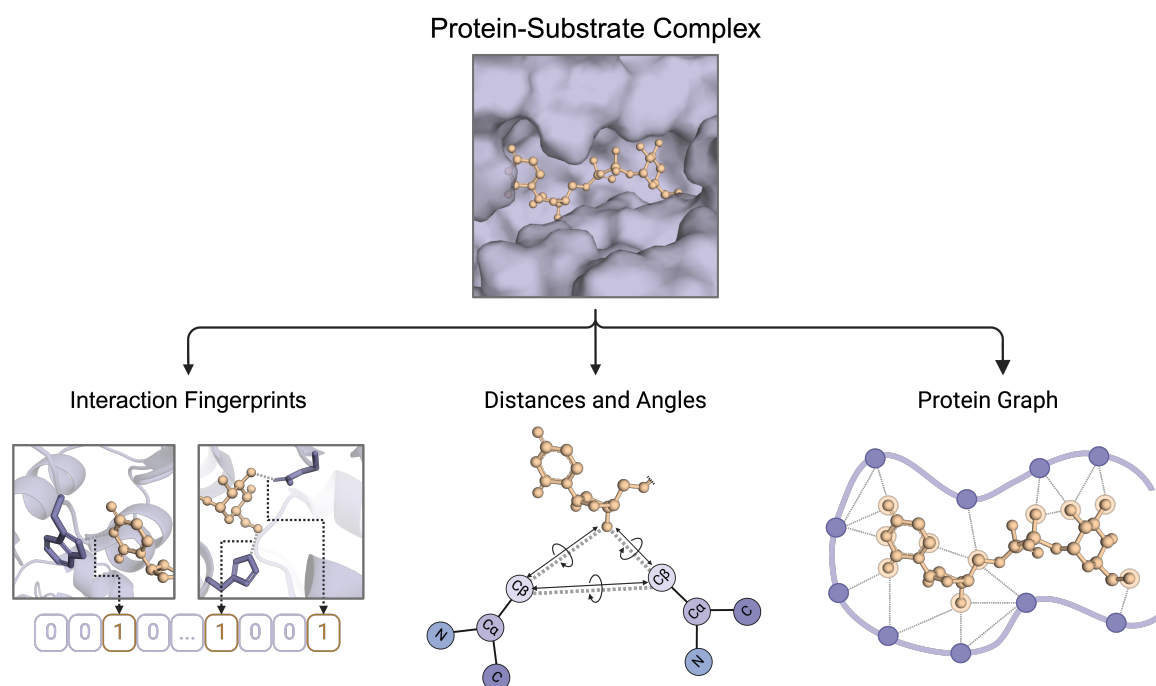
834

835 **5.1 Molecular Docking-based Descriptors and Binding Energies**

836

837 One strategy to generate descriptors of the protein-substrate binding involves the use of
838 scoring functions derived from the docking. For example, the scoring functions from Rosetta
839 (Davis and Baker, 2009; Meiler and Baker, 2006) can be combined with physicochemical and
840 active site descriptors to train a model that can predict the substrate scope of bacterial
841 nitrilases (Mou et al., 2021). The scoring functions described interfacial interaction energy
842 terms including full-atom van der Waals attraction, electrostatics, van der Waals repulsion,
843 hydrogen bonding terms, and solvation energy. From all the features used to train the random
844 forest model, the attractive part of the Lennard-Jones potential obtained from the molecular
845 docking scoring functions was revealed to be the most consistently important variable for the
846 model's performance. A similar approach has been employed to predict the site of
847 metabolism for cytochrome P450 monooxygenases and their substrates in multiple instances
848 (Feng et al., 2023; Huang et al., 2013; Zaretski et al., 2013, 2011). One example included the
849 use of substrate interaction-based descriptors derived from Autodock Vina (Eberhardt et al.,
850 2021; Trott and Olson, 2010) along with chemical reactivity descriptors to train a multiple-

851 instance ranking algorithm (Huang et al., 2013). The model was then used to predict the site
852 of metabolism of the substrates of two cytochrome P450 enzymes, yielding an accuracy of
853 the top two predicted rank positions of 86 % and 83 %, respectively for the two isoforms.
854



855 **Fig. 6. Approaches for encoding the protein-substrate complexes.** The protein-substrate complex can be
856 encoded based on the intermolecular interactions into a binary string commonly denoted as a fingerprint (left).
857 The complex can also be represented by the dihedral angles and distances between catalytic residues along with
858 the angles and distances between catalytic residues and the substrate (middle). Lastly, the protein-substrate
859 complex can be converted into a graph representation where the nodes represent the atoms and the edges
860 represent the interaction between two atoms (right). Notably, while not shown, the complexes can also be
861 represented using scoring functions.
862

863
864 A slightly different route was taken in a study of the bile acid specificity in a single bile acid
865 hydrolase (WT and two mutational variants) (Karlov et al., 2023). Here, a previously
866 published complex of the bile acid hydrolase and a bile acid was used as a template to model
867 the complex with other bile acid substrates with MD simulations. The last nanosecond of a
868 100 ns simulation was used for binding energy calculations employing molecular mechanics
869 Poisson-Boltzmann surface area and molecular mechanics generalized Born surface area
870 methods implemented in AmberTools (Case et al., 2023). The calculated binding energies
871 were then correlated with the corresponding activity data using linear regression which led to
872 the identification of structural determinants of substrate binding and specificity.
873

874 5.2 Interaction fingerprinting

875

876 Another way of representing protein-substrate interactions is through interaction
877 fingerprinting which captures the protein-substrate interactions in one-dimensional binary
878 representations (Figure 6) (Desaphy et al., 2013). This method was utilized for predicting
879 kinase inhibitors by comparing models trained on ligand-interaction fingerprints with models
880 trained on molecular fingerprints of the substrates (Witek et al., 2014). Here, the models
881 trained on the interaction fingerprints outperformed the models trained on molecular
882 fingerprints in discriminating between active and inactive compounds. The use of interaction
883 fingerprints was also explored in a model trained to predict the ligand affinity of HIV-1

884 protease inhibitors (Leidner et al., 2019). The authors extracted interaction fingerprints from
885 crystallized protein-substrate complexes harvested from the Protein Data Bank (Berman et
886 al., 2000), adapting the binary encoding into continuous features describing selected non-
887 covalent interactions. These interaction fingerprints were used to train a gradient-boosting
888 model achieving an RMSE of 1.48 kcal/mol. The study also demonstrated the interpretability
889 of the model using Shapley values which elucidated that van der Waals interactions were
890 critical for model performance.

891

892 **5.3 Distance and Angle-based Representations**

893

894 An alternative encoding strategy for protein-substrate complexes is the use of distances and
895 angles between the substrate and surrounding residues (Figure 6). This was leveraged in a
896 study of hydrolases for the breakdown of several classes of substrates (Ran et al., 2023).
897 Here, the authors aimed to construct a model that could predict the hydrolytic activation free
898 energy for the reactive complexes of hydrolase-catalyzed reactions along with the favored
899 enantiomer of the product. The ability to predict the enantiomeric outcome was enabled by
900 including an atomic distance map consisting of atomic distances between a docked substrate
901 and the C α atoms of the surrounding catalytic residues transformed into a tensor by a single-
902 layer CNN. This map was concatenated with the dihedral angles of the docked substrate
903 converted into sine and cosine values. Combined with sequence-based representations and
904 substrate SMILES, this model could classify reactive and unreactive poses achieving an AUC
905 of 0.87 and a good Pearson R value of 0.72. The model predicted the enantiomeric preference
906 with an accuracy of 55 %. Distances and angles between substrate and enzyme were also
907 employed in a study of ketol-acid reductoisomerases (Bonk et al., 2019). The 68 generated
908 features, consisting of distances and angles between catalytic residues, substrate, cofactor,
909 and active site waters, and magnesium ions, were regularised using LASSO regression, fed to
910 a logistic classifier, and subsequently clustered. The trained model could differentiate
911 between reactive and almost-reactive trajectories with >85 % accuracy. Furthermore, ranking
912 the features from LASSO enabled the identification of a subpart of the reactive site to be
913 particularly important in describing the activity of the enzyme.

914

915 **5.4 Graph Neural Networks for Protein-Substrate Interactions**

916

917 Lately, GNNs have been readily employed to capture detailed information from the protein-
918 substrate complex by converting the docking pose into a graph representation where the
919 nodes represent the atoms and the edges represent their interaction (Yang et al., 2023). This
920 could include the interaction between protein and substrate, between protein and protein, and
921 between substrate and substrate (Figure 6) (Lu et al., 2023; Xia et al., 2023). While not in the
922 realm of biocatalysis, this technique has been used to improve the accuracy of scoring
923 functions of molecular docking (Wang et al., 2022; L. Yang et al., 2021) and to predict
924 protein-ligand affinities (Mastropietro et al., 2023; Wang et al., 2023), especially within drug
925 discovery (Z. Yang et al., 2022). Since enzymes do not solely rely on binding affinity for
926 their functionality, one cannot draw direct parallels between the use of GNNs in these cases
927 and in the case of predicting/understanding the substrate scope of enzymes. However, one
928 study used a GNN-based model to predict and interpret the substrate specificity of multiple
929 mutational variants of two model proteases (Lu et al., 2023). This was achieved by
930 developing a protein graph convolutional network that could model protein structures and
931 their complexes as fully connected graphs where each node corresponded to an amino acid
932 from either the protein or the peptide-substrate while the edges represent the pairwise residue
933 interactions between the nodes. The generated model could ultimately predict protease

934 activity with a given substrate achieving an accuracy >85 % across protease variants. In
935 addition, the authors also displayed how node and edge ablation tests provided insights into
936 the feature importance of the models. In a model that only included sequence-based features,
937 the edges did not affect the model accuracy, and the peptide nodes played a leading role.
938 However, when energy-based features were included, ablating edge-based features
939 significantly impacted the model accuracy with the intermolecular edges being particularly
940 important.

941
942 Overall, the use of protein-substrate complexes to generate representations holds great
943 promise within ML for biocatalytic systems. Many of the described methods capture
944 interpretable information which is useful in cases where explainability is an important factor.
945 However, one should still keep in mind that obtaining protein-substrate complexes is
946 computationally demanding when using molecular docking, making the method realistic for
947 smaller datasets, at least until the ML-based docking methods significantly accelerate the
948 process (Buttenschoen et al., 2024). In addition, molecular docking is not an accurate method,
949 especially without manual inspection of poses, which could directly impact the accuracy of
950 the model.

951 952 **6. Choosing a Suitable Representation**

953
954 Selecting the most appropriate representation approach when constructing models can be a
955 challenging task, and although several attempts have been made to examine the efficacies of
956 different encoding techniques (Elabd et al., 2020; Goldman et al., 2022; Michael et al., 2023;
957 Bruce J. Wittmann et al., 2021), no consensus exists for determining the best representation
958 for a new protein ML model. Consequently, finding a suitable protein representation remains
959 case-dependent. To address this issue, we propose two general factors to consider (Figure 7).
960 The first factor is the model setup, determining the overall design of the predictive tool. This
961 includes the size of the training dataset, defining the ease of discovering hidden patterns, and
962 the choice of ML architecture, imposing requirements for the input representation. The
963 second factor is the model objective, describing the type of task envisioned for the resulting
964 model. Linking the choice of representation with project objectives such as the assayed
965 property, wild type vs. mutational predictor, and explainability may eventually increase the
966 chances of achieving these objectives. We expect that these two factors can be used as a
967 source of inspiration and guidance when creating new ML models for biocatalysis.

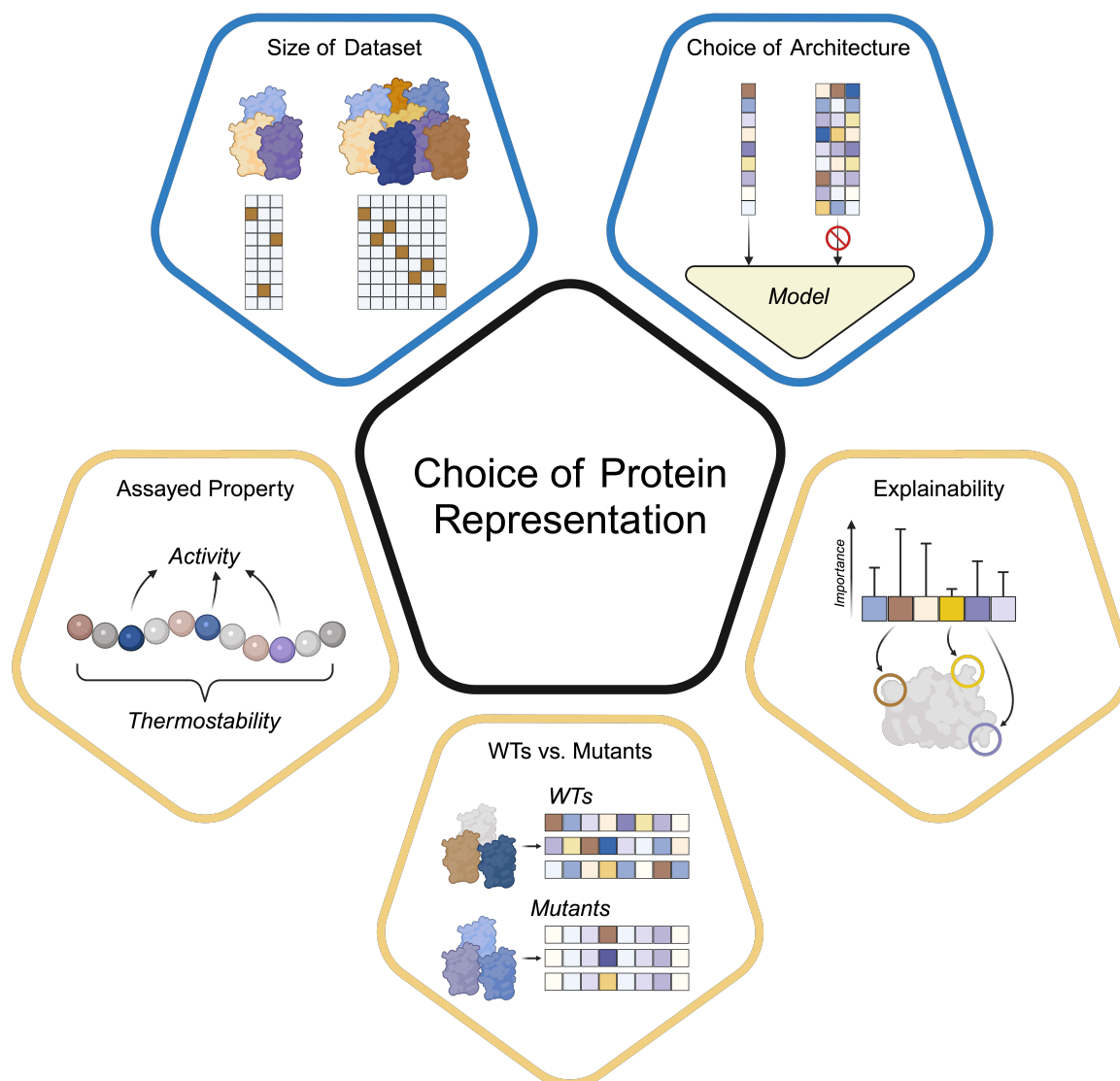
968 969 **6.1 Model Setup**

970
971 When developing an ML model, design decisions are often made based on element harmony,
972 where the size of the dataset matches the model architecture. This is also applicable to the
973 choice of a suitable protein representation, and selecting a harmonious encoding strategy
974 based on the model setup is extremely important. In this section, we will discuss how model
975 design can influence the appropriate representation approach.

976 977 **6.1.1 Size of Dataset**

978
979 An important feature of the model setup is the size of the dataset. Here, a protein
980 representation approach that produces a large feature set might be problematic when
981 encoding smaller data sets due to a poor data-to-feature ratio, as the high dimensionality
982 introduces sparsity and higher chances of finding patterns in feature noise. This can lead to
983 significant overfitting, thus hindering the identification of hidden patterns and trends in the

984 data which is crucial for an efficient and accurate predictive model (Bellman, 1961;
985 Theodoridis and Koutroumbas, 2008). The low-to-medium-throughput nature of experiments
986 is a common issue in biocatalysis, which imposes significant restrictions on the choice of
987 suitable representations for ML to ensure only informative features are incorporated.
988



989 **Fig. 7. Factors influencing the choice of a suitable protein representation.** The first main factor is “model
990 setup” (colored blue), which concerns the size of the dataset due to small datasets potentially preventing the
991 discovery of patterns contained in sparse representations. The choice of ML architecture might instead impede
992 the use of certain representations due to incompatibility. The second main factor is “model objective” (colored
993 beige), as specialized representation might enhance models for predicting assayed enzyme properties such as
994 activity, while full representations will likely better suit global properties, *e.g.*, thermostability. Furthermore,
995 WT models impose different requirements on the encoding strategy than mutant predictors due to the disparity
996 in representation similarity. Finally, any explainability task will benefit from a clear connection between the
997 model features and protein features.
998
999

1000 A promising strategy to circumvent this problem is to leverage the large pre-trained models
1001 for self-supervised representation learning (Ferruz and Höcker, 2022; Notin et al., 2023; Qiu
1002 and Wei, 2023). A notable example of this is the approach introduced by Biswas et al., which
1003 involved fine-tuning the deep neural network UniRep by using the sequences evolutionarily
1004 related to their protein of interest, GFP, thus adapting the resulting latent vector embeddings

1005 to better encode protein information crucial to the evolution of GFP (Biswas et al., 2021).
1006 The resulting ML models were capable of identifying mutants with increased fluorescence
1007 using as few as 24 mutants as training data. Biswas et al. observed a large sequence diversity
1008 in the new model-based variants, suggesting that the increased density of evolutionary
1009 important information contained in the protein representation due to the fine-tuning
1010 procedure allowed for a greater exploration of the sequence-to-function space.

1011
1012 Related to utilizing knowledge from pre-trained embeddings, insights obtained from a
1013 mutational study of a single enzyme can be transferred to homologues with little
1014 characterization. This is known as transfer learning which entails training models on large
1015 datasets to study scarce datasets (Yosinski et al., 2014). This could eliminate the requirement
1016 of conducting a thorough mutational assay every time a new enzyme is examined and
1017 facilitate Low-N modeling, though this is yet to be explored for biocatalysis.

1018
1019 Alleviating the issue of a low amount of data can be done with the previously mentioned
1020 approach of augmenting a VAE-based evolutionary density score with a simple OHE (Hsu et
1021 al., 2022). Models trained on as few as 48 proteins exhibited good performance when
1022 utilizing this augmentation technique. This finding highlights how combining representations
1023 containing different protein information can be beneficial.

1024
1025 Notably, while a low amount of data is a significant hindrance for most encoding strategies, a
1026 large dataset might instead hinder the use of representations requiring significant processing
1027 power. This includes methods for QM calculations or MD simulations, as their computational
1028 demands make them infeasible for datasets with a large selection of proteins. This might be
1029 especially relevant for predictive models trained on dynamics representations, as the
1030 acquisition of such protein encodings is often computationally expensive, introducing a
1031 question of balance between a larger dataset and an increased usage of computational
1032 resources.

1033
1034 Lastly, while the size of the training dataset is extremely influential for the choice of suitable
1035 representation, another important related step is the split between test and training data. Here,
1036 the choice of representation influences the preferred approach for cross-validation due to the
1037 different types of information bias (Corso et al., 2024; Kanakala et al., 2022; Kroll and
1038 Lercher, 2023; J. Li et al., 2023). It is important to harmonize the dataset validation strategy
1039 with the protein representation.

1040 1041 **6.1.2 Choice of Architecture**

1042
1043 Even though the choice of model architecture is often related to the amount of training data
1044 available due to how the performance of ML algorithms often depends on the size of the
1045 dataset (Beleites et al., 2012; Raudys and Jain, 1991), the architecture imposes different
1046 requirements to the representation than those described in the previous section. While
1047 innumerable ML architectures have been developed, researchers are more likely to build
1048 models inside of their field of expertise. Therefore, the model architecture is often determined
1049 before the encoding approach, and the choice of protein representation is therefore strongly
1050 influenced by the model architecture. Classical ML methods, such as logistic regression,
1051 KNN, and random forest, usually require a 1D vector with numerical values. Consequently,
1052 any multidimensional information must either be flattened or reduced in dimensions before
1053 use in these models, potentially losing the important data structure contained in the
1054 representation. Employing a representation with a large feature set together with the simplest

1055 of architectures might also cause problems due to their limited capacity to discover the
1056 patterns in the feature set.

1057

1058 Some protein representations might require the use of advanced DL architectures such as
1059 GNNs and CNNs as highlighted in the description of structure representations. If a
1060 researcher's field of expertise is mainly CNNs, combining these ML architectures with a
1061 protein voxel representation is likely more beneficial than attempting to employ protein
1062 graphs and GNNs. Consequently, the generalisability of fixed descriptors is quite
1063 advantageous.

1064

1065 Finally, some ML models have shown dispositions towards memorization instead of
1066 generalization (Buttenschoen et al., 2024; Corso et al., 2024; Kroll and Lercher, 2023;
1067 Wallach and Heifets, 2018). Rather than learning a fundamental relationship between the
1068 proteins and their function through the model features, they memorize all individual
1069 representations in the training set which leads to a high degree of overfitting. If the chosen
1070 architecture tends to achieve high validation accuracy due to such memorization, we propose
1071 to employ fixed encoding strategies instead of learned representation. This is due to the latter
1072 often behaving as a fingerprint with few similarities between two representations, while a set
1073 of proteins encoded with fixed representations often has the same values across different
1074 descriptors. In consequence, the model will be less likely to turn towards memorization when
1075 these fixed features are used.

1076

1077 **6.2 Model Objective**

1078

1079 The second factor that influences the choice of suitable protein representation is the objective
1080 envisioned for the ML model. Certain enzyme properties might benefit from using
1081 specialized representation methods. Another important distinction comes from the contrast
1082 between training models on WT and mutational data. Finally, we will discuss tasks in which
1083 explainability is essential.

1084

1085 **6.2.1 Assayed Property**

1086

1087 If the objective of the model is to examine the activity or specificity of the enzymes, it is
1088 crucial to encode the active site — potentially only focusing on the area of the protein
1089 containing this site. In our recent model for glycosyltransferase acceptor specificity
1090 predictions, we limited the representation to contain only the N-terminal domain which
1091 contains the acceptor binding site (Harding-Larsen et al., 2023). The structure-informed ASC
1092 method also allowed Röttig et al. to focus the representation on the active site (Röttig et al.,
1093 2010). Other examples of the representations targeting task-specific parts of the protein
1094 include the domain embeddings of Domain-PFP for predicting Gene Ontology (GO)
1095 annotations (Ibtehaz et al., 2023), the site embeddings and encoding of neighbouring regions
1096 N-linked glycosylation site predictions in EMNGly (Hou et al., 2023), and the
1097 microenvironments of MutCompute used for identifying position where mutations can
1098 stabilize the local environment (Paik et al., 2023; Shroff et al., 2020).

1099

1100 However, as previously described, limiting the representation to specific areas of the protein
1101 can potentially remove important information, such as for allostery or protein fitness. To
1102 capture this information, a more general protein encoding will be more suitable to allow the
1103 resulting ML model to explore the entire sequence and structure landscape.

1104

1105 6.2.2 Wild Type vs Mutational Data

1106

1107 Aside from predicted property, the type of enzymes, be it mutants or wild-type (WT)
1108 proteins, will also significantly influence the choice of representation as two variants of the
1109 same enzyme are inherently more similar than two WT proteins from the same family. An
1110 ML model trained on mutant data can thus utilize more specialized protein representations
1111 than a model trained on WT data due to a significant portion of the sequence being constant
1112 across every variant. This strategy was employed by Saito et al. to encode variants of Sortase
1113 A for use in MLDE by only encoding five positions known to result in a high-activity variant,
1114 ultimately achieving an improved variant of the enzyme (Saito et al., 2021). Such an
1115 approach will not be possible for a WT predictor, as not only will large portions of the
1116 proteins potentially differ, but the length of each protein is unlikely to be equal.

1117

1118 Due to the limited variance contained in the sequences of mutant datasets, the representation
1119 strategies require higher sensitivity to the minute changes between each variant. Otherwise,
1120 the resulting ML model will be unable to discern top-performing variants from those of poor
1121 nature. Unfortunately, no gold standard has been established for the sensitivity of encoding
1122 techniques, and it is therefore difficult to determine the best representation strategy in this
1123 endeavour. Wittmann et al. proposed that learned embeddings obtained from models trained
1124 on MSAs will result in representations containing a higher density of information important
1125 for mutational tasks due to highlighting which mutations are evolutionarily feasible (Bruce J.
1126 Wittmann et al., 2021). Nevertheless, they only observed small performance increases when
1127 using embeddings from MSA Transformer (Rao et al., 2021), highlighting how a suitable
1128 representation can be highly case-dependent. Consequently, new representation learning
1129 models should be benchmarked through large collections of diverse datasets such as the deep
1130 mutational scans collected in ProteinGym (Notin et al., 2023).

1131

1132 WT models do not have the same sensitivity issue due to the larger variance between the
1133 training sequences. This is of course by design, as WT models often remove proteins within a
1134 preset similarity cutoff. Instead, the representation of WT proteins introduces a question of
1135 compatibility across all proteins in both the training and test data. Methods requiring
1136 sequence alignments, such as OHE, BLOSUM encodings, or structure-informed approaches,
1137 will not work with sequences of low similarity. Here, graph models trained on structurally
1138 heterogeneous enzymes might be superior.

1139

1140 6.2.3 Explaining Protein Representations

1141

1142 In some studies, the model objective is mainly to produce a predictive model that can be
1143 utilized for future *in silico* scoring of potential variants or WT enzymes for a given reaction.
1144 In that case, the representation strategy producing the highest accuracy is likely desired.
1145 However, if the purpose of the model is instead to obtain a fundamental understanding of the
1146 forces governing the protein function and the modeled process, the explainability of the
1147 model is crucial.

1148

1149 Recently, the notion of Explainable AI (XAI) has gained momentum, with terms such as
1150 explainability, interpretability, and justification being regarded as increasingly valuable for
1151 new models (Novakovsky et al., 2022; Vilone and Longo, 2020; Wellawatte et al., 2023;
1152 Wojciech Samek et al., 2019). In ML for biocatalysis, the ability to explain model decisions
1153 actively allows a more thorough understanding of enzyme features and phenotypes. However,
1154 as XAI mainly addresses the *model* features, the accuracy of said explanations depends on the

1155 connection between model features and protein properties — a connection, that is defined by
1156 the encoding strategy.

1157
1158 If the model features represent inherent amino acid characteristics such as physicochemical
1159 properties, incorporation of XAI can help pinpoint which of these residue features are
1160 important for model predictions. This knowledge may lead to novel insights as well as
1161 potentially assist in choosing targets for the rational design of new variants with enhanced
1162 enzymatic properties. XAI was utilized by Robinson et al. to elucidate the essential residues
1163 for the activity of thiolase members of the OleA enzyme family (Robinson et al., 2020) and
1164 by Tadjale et al. to discover a buried residue important for the donor specificity of fold A
1165 glycosyltransferases (Tadjale et al., 2020).

1166
1167 If coarse-grained protein properties are implemented in the model features, the ability to
1168 identify important amino acid attributes is reduced. Here, the implementation of XAI can
1169 instead be utilized to compare the influence of the different protein characteristics, an
1170 approach taken by Heckman et al. to highlight the importance of structural properties for the
1171 activity of metabolic enzymes at the genome scale (Heckmann et al., 2020, 2018), as well as
1172 by Mou et al. (Mou et al., 2021) and Carlin et al. (Carlin et al., 2016) to identify key ligand
1173 binding-related features for nitrilase substrate specificity and glycoside hydrolase kinetics,
1174 respectively.

1175
1176 Finally, encoding the protein using learned embeddings introduces some interesting
1177 challenges in XAI, as the abstract representation often does not translate directly to specific
1178 properties in the protein. Consequently, explaining the protein properties based on the
1179 importance of the model features is even more complicated than for the coarse-grained
1180 representations. One solution is to use an attention mechanism when constructing the protein
1181 embeddings, as implemented by Li et al. when examining the positional importance with
1182 regard to the k_{cat} of WT metabolic enzymes (Li et al., 2022). Due to the DL nature of their
1183 model architecture, they would have been unable to directly extract the feature importance of
1184 their model (Wellawatte et al., 2023; Wojciech Samek et al., 2019). Here, the authors
1185 incorporated an additional sub-architecture, the attention mechanism, that allows the model to
1186 “remember” the connection between input properties and embedding features (Bahdanau et
1187 al., 2014; Li et al., 2022; Wellawatte et al., 2023).

1188
1189 Instead of changing the architecture, the model decisions can also be elucidated using input
1190 perturbation such as *in silico* mutagenesis, where the input sequence is perturbed by changing
1191 a single amino acid and then examining the difference between the model prediction of the
1192 original and new sequence (Novakovsky et al., 2022; Zhou and Troyanskaya, 2015). This
1193 difference, also known as the attribution score (Novakovsky et al., 2022), can then be
1194 calculated for a large number of perturbations, ideally, all possible ones, resulting in a
1195 thorough sequence-function landscape of the ML model. This landscape can be examined to
1196 determine the key residue properties, thus introducing explainability to an inherently abstract
1197 protein representation and modeling approach.

1198 1199 **7. Summary & Outlook**

1200
1201 In this review, we have presented a diverse selection of the most prominent strategies for
1202 encoding enzyme information for ML modeling. The representation approaches are capable
1203 of utilizing varying levels of protein information, from primary sequence to temporal
1204 dynamics, and their complexities range from fixed descriptors with little inherent bias to

1205 learned presentations extracted from complex DL models. To navigate this ever-growing
1206 field, we introduced two main factors for choosing the most suitable encoding strategy:
1207 “model setup”, especially concerning the training dataset size and ML architecture, and
1208 “model objective”, relating to the assayed enzyme property, the differences between a WT
1209 model and mutant predictor, and explainability of the model. We believe that this review
1210 serves as both a source of information and a guide for future researchers in biocatalysis when
1211 determining a suitable encoding strategy for their own ML models. The field is rapidly
1212 expanding, and we envision a promising future for the development and use of more
1213 sophisticated protein encodings. Solving the Low-N objective is a pressing objective, and
1214 future approaches should build on the pioneering work of fine-tuning pre-trained PLM
1215 embeddings or the combination of representations containing distinct information and
1216 inherent bias. Another vital task is to efficiently incorporate protein dynamics representations
1217 due to their ability to capture crucial aspects of enzymatic behavior. Lastly, we hope that
1218 future ML projects for biocatalysis will ensure a better alignment between the choice of
1219 protein representation and model design.

1220

1221 **Acknowledgments**

1222 We thank The Novo Nordisk Foundation for supporting this work through grant
1223 NNF20CC0035580. This work was also supported by Czech Ministry of Education, Youth
1224 and Sports [CETOCOEN Excellence CZ.02.1.01/0.0/0.0/17_043/0009632, ESFRI
1225 RECETOX RI LM2023069, ESFRI ELIXIR LM2023055] and the CETOCOEN
1226 EXCELLENCE Teaming 2 project supported by Horizon2020 of the European Union
1227 [857560].

1228 Figures were created with BioRender.com

1229

1230 **Declaration of Competing Interest**

1231 The authors declare no competing interests.

1232 **References**

- 1233
- 1234 Acevedo-Rocha, C.G., Gamble, C.G., Lonsdale, R., Li, A., Nett, N., Hoebenreich, S.,
 1235 Lingnau, J.B., Wirtz, C., Fares, C., Hinrichs, H., Deege, A., Mulholland, A.J., Nov, Y.,
 1236 Leys, D., McLean, K.J., Munro, A.W., Reetz, M.T., 2018. P450-Catalyzed regio- and
 1237 diastereoselective steroid hydroxylation: Efficient directed evolution enabled by
 1238 mutability landscaping. *ACS Catal* 8, 3395–3410.
 1239 [https://doi.org/10.1021/ACSCATAL.8B00389/ASSET/IMAGES/LARGE/CS-2018-](https://doi.org/10.1021/ACSCATAL.8B00389/ASSET/IMAGES/LARGE/CS-2018-003898_0005.JPG)
 1240 [003898_0005.JPG](https://doi.org/10.1021/ACSCATAL.8B00389/ASSET/IMAGES/LARGE/CS-2018-003898_0005.JPG)
- 1241 Acevedo-Rocha, C.G., Li, A., D'Amore, L., Hoebenreich, S., Sanchis, J., Lubrano, P., Ferla,
 1242 M.P., Garcia-Borràs, M., Osuna, S., Reetz, M.T., 2021. Pervasive cooperative
 1243 mutational effects on multiple catalytic enzyme traits emerge via long-range
 1244 conformational dynamics. *Nat Commun* 12. [https://doi.org/10.1038/s41467-021-21833-](https://doi.org/10.1038/s41467-021-21833-w)
 1245 [w](https://doi.org/10.1038/s41467-021-21833-w)
- 1246 Agarwal, P.K., Bernard, D.N., Bafna, K., Doucet, N., 2020. Enzyme dynamics: Looking
 1247 beyond a single structure. *ChemCatChem* 12, 4704–4720.
 1248 <https://doi.org/10.1002/cctc.202000665>
- 1249 Ahdritz, G., Bouatta, N., Kadyan, S., Xia, Q., Gerecke, W., O, T.J., Berenberg, D., Fisk, I.,
 1250 Zanichelli, N., Zhang, B., Nowaczynski, A., Wang, B., Stepniewska-Dziubinska, M.M.,
 1251 Zhang, S., Ojewole, A., Efe Guney, M., Biderman, S., Watkins, A.M., Ra, S., Ribalta
 1252 Lorenzo, P., Nivon, L., Weitzner, B., Andrew Ban, Y.-E., Sorger, P.K., Mostaque, E.,
 1253 Zhang, Z., Bonneau, R., AlQuraishi, M., Allen Hamilton, B., Bio, C., 2022. OpenFold:
 1254 Retraining AlphaFold2 yields new insights into its learning mechanisms and capacity for
 1255 generalization. *bioRxiv* 2022.11.20.517210. <https://doi.org/10.1101/2022.11.20.517210>
- 1256 Ainsley, J., Mulholland, A.J., Black, G.W., Sparagano, O., Christov, C.Z., Karabencheva-
 1257 Christova, T.G., 2018. Structural Insights from Molecular Dynamics Simulations of
 1258 Tryptophan 7-Halogenase and Tryptophan 5-Halogenase. *ACS Omega* 3, 4847–4859.
 1259 <https://doi.org/10.1021/acsomega.8b00385>
- 1260 Altschul, S.F., Madden, T.L., Schäffer, A.A., Zhang, J., Zhang, Z., Miller, W., Lipman, D.J.,
 1261 1997. Gapped BLAST and PSI-BLAST: a new generation of protein database search
 1262 programs. *Nucleic Acids Res* 25, 3389–3402. <https://doi.org/10.1093/NAR/25.17.3389>
- 1263 A.Maria-Solano, M., Serrano-Hervás, E., Romero-Rivera, A., Iglesias-Fernández, J., Osuna,
 1264 S., 2018. Role of conformational dynamics in the evolution of novel enzyme function.
 1265 *Chemical Communications* 54, 6622–6634. <https://doi.org/10.1039/C8CC02426J>
- 1266 Amidi, A., Amidi, S., Vlachakis, D., Megalooikonomou, V., Paragios, N., Zacharaki, E.I.,
 1267 2018. EnzyNet: enzyme classification using 3D convolutional neural networks on spatial
 1268 representation. *PeerJ* 6. <https://doi.org/10.7717/PEERJ.4750>
- 1269 Ao, Y.F., Dörr, M., Menke, M.J., Born, S., Heuson, E., Bornscheuer, U.T., 2024. Data-
 1270 Driven Protein Engineering for Improving Catalytic Activity and Selectivity.
 1271 *Chembiochem* 25. <https://doi.org/10.1002/CBIC.202300754>
- 1272 Arnold, F.H., 2018. Directed Evolution: Bringing New Chemistry to Life. *Angew Chem Int*
 1273 *Ed Engl* 57, 4143. <https://doi.org/10.1002/ANIE.201708408>
- 1274 Arnold, F.H., 1998. Design by Directed Evolution. *Acc Chem Res* 31, 125–131.
 1275 <https://doi.org/10.1021/AR960017F/ASSET/IMAGES/LARGE/AR960017FF00005.JPG>
 1276 [G](https://doi.org/10.1021/AR960017F/ASSET/IMAGES/LARGE/AR960017FF00005.JPG)
- 1277 Arnold, F.H., 1996. Directed evolution: Creating biocatalysts for the future. *Chem Eng Sci*
 1278 51, 5091–5102. [https://doi.org/10.1016/S0009-2509\(96\)00288-6](https://doi.org/10.1016/S0009-2509(96)00288-6)
- 1279 Arts, M., Frelsen, J., Boomsma, W., 2023. Internal-Coordinate Density Modelling of Protein
 1280 Structure: Covariance Matters. *ArXiv*.

1281 Atchley, W.R., Zhao, J., Fernandes, A.D., Druke, T., 2005. Solving the protein sequence
1282 metric problem. *Proc Natl Acad Sci U S A* 102, 6395–6400.
1283 https://doi.org/10.1073/PNAS.0408677102/SUPPL_FILE/08677TABLE5.XLS
1284 Audagnotto, M., Czechtizky, W., De Maria, L., Käck, H., Papoian, G., Tornberg, L.,
1285 Tyrchan, C., Ulander, J., 2022. Machine learning/molecular dynamic protein structure
1286 prediction approach to investigate the protein conformational ensemble. *Sci Rep* 12,
1287 10018. <https://doi.org/10.1038/s41598-022-13714-z>
1288 Baek, M., DiMaio, F., Anishchenko, I., Dauparas, J., Ovchinnikov, S., Lee, G.R., Wang, J.,
1289 Cong, Q., Kinch, L.N., Dustin Schaeffer, R., Millán, C., Park, H., Adams, C., Glassman,
1290 C.R., DeGiovanni, A., Pereira, J.H., Rodrigues, A. V., Van Dijk, A.A., Ebrecht, A.C.,
1291 Opperman, D.J., Sagmeister, T., Buhlheller, C., Pavkov-Keller, T., Rathinaswamy,
1292 M.K., Dalwadi, U., Yip, C.K., Burke, J.E., Christopher Garcia, K., Grishin, N. V.,
1293 Adams, P.D., Read, R.J., Baker, D., 2021. Accurate prediction of protein structures and
1294 interactions using a three-track neural network. *Science* (1979) 373, 871–876.
1295 https://doi.org/10.1126/SCIENCE.ABJ8754/SUPPL_FILE/ABJ8754_MDAR_REPROD
1296 [UCIBILITY_CHECKLIST.PDF](https://doi.org/10.1126/SCIENCE.ABJ8754/SUPPL_FILE/ABJ8754_MDAR_REPROD)
1297 Bahdanau, D., Cho, K.H., Bengio, Y., 2014. Neural Machine Translation by Jointly Learning
1298 to Align and Translate. 3rd International Conference on Learning Representations, ICLR
1299 2015 - Conference Track Proceedings.
1300 Baxter, J., 2000. A model of inductive bias learning. *Journal of artificial intelligence research*
1301 12, 149–198.
1302 Behera, S., Balasubramanian, S., 2023. Lipase A from *Bacillus subtilis*: Substrate Binding,
1303 Conformational Dynamics, and Signatures of a Lid. *J. Chem. Inf. Model.*
1304 <https://doi.org/10.1021/acs.jcim.3c01681>
1305 Beleites, C., Neugebauer, U., Bocklitz, T., Krafft, C., Popp, J., 2012. Sample Size Planning
1306 for Classification Models. *Anal Chim Acta* 760, 25–33.
1307 <https://doi.org/10.1016/j.aca.2012.11.007>
1308 Bellman, R., 1966. Dynamic programming. *Science* (1979) 153, 34–37.
1309 Bellman, R., 1961. Adaptive control processes : a guided tour. Princeton University Press.
1310 Bengio, Y., Courville, A., Vincent, P., 2013. Representation learning: A review and new
1311 perspectives. *IEEE Trans Pattern Anal Mach Intell* 35, 1798–1828.
1312 Berman, H.M., Westbrook, J., Feng, Z., Gilliland, G., Bhat, T.N., Weissig, H., Shindyalov,
1313 I.N., Bourne, P.E., 2000. The Protein Data Bank. *Nucleic Acids Res* 28, 235–242.
1314 <https://doi.org/10.1093/NAR/28.1.235>
1315 Berselli, A., Ramos, M.J., Menziani, M.C., 2021. Novel Pet-Degrading Enzymes: Structure-
1316 Function from a Computational Perspective. *Chembiochem* 22, 2032–2050.
1317 <https://doi.org/10.1002/CBIC.202000841>
1318 Bhakat, S., 2022. Collective variable discovery in the age of machine learning: reality, hype
1319 and everything in between. *RSC Adv* 12, 25010. <https://doi.org/10.1039/D2RA03660F>
1320 Bhattacharya, S., Margheritis, E.G., Takahashi, K., Kulesha, A., D'Souza, A., Kim, I., Yoon,
1321 J.H., Tame, J.R.H., Volkov, A.N., Makhlynets, O. V, Korendovych, I. V, 2022. NMR-
1322 guided directed evolution. *Nature* 610, 389–393. <https://doi.org/10.1038/s41586-022->
1323 [05278-9](https://doi.org/10.1038/s41586-022-05278-9)
1324 Bilal, M., Adeel, M., Rasheed, T., Zhao, Y., Iqbal, H.M.N., 2019. Emerging contaminants of
1325 high concern and their enzyme-assisted biodegradation – A review. *Environ Int* 124,
1326 336–353. <https://doi.org/10.1016/J.ENVINT.2019.01.011>
1327 Biswas, S., Khimulya, G., Alley, E.C., Esvelt, K.M., Church, G.M., 2021. Low-N protein
1328 engineering with data-efficient deep learning. *Nature Methods* 2021 18:4 18, 389–396.
1329 <https://doi.org/10.1038/s41592-021-01100-y>

1330 Blaabjerg, L.M., Kassem, M.M., Good, L.L., Jonsson, N., Cagiada, M., Johansson, K.E.,
1331 Boomsma, W., Stein, A., Lindorff-Larsen, K., 2023. Rapid protein stability prediction
1332 using deep learning representations. *Elife* 12. <https://doi.org/10.7554/ELIFE.82593>
1333 Bonk, B.M., Weis, J.W., Tidor, B., 2019. Machine Learning Identifies Chemical
1334 Characteristics That Promote Enzyme Catalysis. *J Am Chem Soc* 141, 4108–4118.
1335 <https://doi.org/10.1021/JACS.8B13879/ASSET/IMAGES/LARGE/JA-2018->
1336 [138797_0003.JPEG](https://doi.org/10.1021/JACS.8B13879/ASSET/IMAGES/LARGE/JA-2018-138797_0003.JPEG)
1337 Bornscheuer, U.T., Pohl, M., 2001. Improved biocatalysts by directed evolution and rational
1338 protein design. *Curr Opin Chem Biol* 5, 137–143. <https://doi.org/10.1016/S1367->
1339 [5931\(00\)00182-4](https://doi.org/10.1016/S1367-5931(00)00182-4)
1340 Bose, A.J., Akhound-Sadegh, T., Fatras, K., Hugué, G., Rector-Brooks, J., Liu, C.-H., Nica,
1341 A.C., Korablyov, M., Bronstein, M., Tong, A., 2023. SE(3)-Stochastic Flow Matching
1342 for Protein Backbone Generation. *ArXiv*.
1343 Brandes, N., Ofer, D., Peleg, Y., Rappoport, N., Linial, M., 2022. ProteinBERT: a universal
1344 deep-learning model of protein sequence and function. *Bioinformatics* 38, 2102–2110.
1345 Broom, A., Rakotoharisoa, R. V, Thompson, M.C., Zarifi, N., Nguyen, E., Mukhametzhanov,
1346 N., Liu, L., Fraser, J.S., Chica, R.A., 2020. Ensemble-based enzyme design can
1347 recapitulate the effects of laboratory directed evolution in silico. *Nat Commun* 11, 4808.
1348 <https://doi.org/10.1038/s41467-020-18619-x>
1349 Buller, R., Lutz, S., Kazlauskas, R.J., Snajdrova, R., Moore, J.C., Bornscheuer, U.T., 2023.
1350 From nature to industry: Harnessing enzymes for biocatalysis. *Science* 382, eadh8615.
1351 <https://doi.org/10.1126/SCIENCE.ADH8615/ASSET/28A24AA3-9B29-4667-82B4->
1352 [E629A9BD74F3/ASSETS/IMAGES/LARGE/SCIENCE.ADH8615-F5.JPG](https://doi.org/10.1126/SCIENCE.ADH8615/ASSET/28A24AA3-9B29-4667-82B4-E629A9BD74F3/ASSETS/IMAGES/LARGE/SCIENCE.ADH8615-F5.JPG)
1353 Bunzel, H.A., Anderson, J.L.R., Hilvert, D., Arcus, V.L., van der Kamp, M.W., Mulholland,
1354 A.J., 2021. Evolution of dynamical networks enhances catalysis in a designer enzyme.
1355 *Nat. Chem.* 13, 1017–1022. <https://doi.org/10.1038/s41557-021-00763-6>
1356 Buttenschoen, M., Morris, G.M., Deane, C.M., 2024. PoseBusters: AI-based docking
1357 methods fail to generate physically valid poses or generalise to novel sequences. *Chem*
1358 *Sci* 15, 3130–3139. <https://doi.org/10.1039/D3SC04185A>
1359 Cadet, F., Fontaine, N., Li, G., Sanchis, J., Ng Fuk Chong, M., Pandjaitan, R., Vetrivel, I.,
1360 Offmann, B., Reetz, M.T., 2018. A machine learning approach for reliable prediction of
1361 amino acid interactions and its application in the directed evolution of enantioselective
1362 enzymes. *Sci Rep* 8. <https://doi.org/10.1038/S41598-018-35033-Y>
1363 Cadet, X.F., Gelly, J.C., van Noord, A., Cadet, F., Acevedo-Rocha, C.G., 2022. Learning
1364 Strategies in Protein Directed Evolution. *Methods Mol Biol* 2461, 225–275.
1365 https://doi.org/10.1007/978-1-0716-2152-3_15
1366 Calvó-Tusell, C., Maria-Solano, M.A., Osuna, S., Feixas, F., 2022a. Time Evolution of the
1367 Millisecond Allosteric Activation of Imidazole Glycerol Phosphate Synthase. *J Am*
1368 *Chem Soc* 144, 7146–7159.
1369 https://doi.org/10.1021/JACS.1C12629/SUPPL_FILE/JA1C12629_SI_003.MP4
1370 Calvó-Tusell, C., Maria-Solano, M.A., Osuna, S., Feixas, F., 2022b. Time Evolution of the
1371 Millisecond Allosteric Activation of Imidazole Glycerol Phosphate Synthase. *J Am*
1372 *Chem Soc* 144, 7146–7159.
1373 https://doi.org/10.1021/JACS.1C12629/SUPPL_FILE/JA1C12629_SI_003.MP4
1374 Calzadiaz-Ramirez, L., Calvó-Tusell, C., Stoffel, G.M.M., Lindner, S.N., Osuna, S., Erb,
1375 T.J., Garcia-Borràs, M., Bar-Even, A., Acevedo-Rocha, C.G., 2020. In Vivo Selection
1376 for Formate Dehydrogenases with High Efficiency and Specificity toward NADP⁺. *ACS*
1377 *Catal* 10, 7512–7525.
1378 https://doi.org/10.1021/ACSCATAL.0C01487/ASSET/IMAGES/LARGE/CS0C01487_
1379 [0008.JPEG](https://doi.org/10.1021/ACSCATAL.0C01487/ASSET/IMAGES/LARGE/CS0C01487_0008.JPEG)

1380 Campbell, E., Kaltenbach, M., Correy, G.J., Carr, P.D., Porebski, B.T., Livingstone, E.K.,
1381 Afriat-Jurnou, L., Buckle, A.M., Weik, M., Hollfelder, F., Tokuriki, N., Jackson, C.J.,
1382 2016. The role of protein dynamics in the evolution of new enzyme function. *Nat Chem*
1383 *Biol* 12, 944–950. <https://doi.org/10.1038/nchembio.2175>
1384 Campbell, E.C., Correy, G.J., Mabbitt, P.D., Buckle, A.M., Tokuriki, N., Jackson, C.J., 2018.
1385 Laboratory evolution of protein conformational dynamics. *Curr Opin Struct Biol* 50, 49–
1386 57. <https://doi.org/10.1016/j.sbi.2017.09.005>
1387 Carlin, D.A., Caster, R.W., Wang, X., Betzenderfer, S.A., Chen, C.X., Duong, V.M.,
1388 Ryklansky, C. V., Alpekin, A., Beaumont, N., Kapoor, H., Kim, N., Mohabbot, H.,
1389 Pang, B., Teel, R., Whithaus, L., Tagkopoulos, I., Siegel, J.B., 2016. Kinetic
1390 Characterization of 100 Glycoside Hydrolase Mutants Enables the Discovery of
1391 Structural Features Correlated with Kinetic Constants. *PLoS One* 11, e0147596.
1392 <https://doi.org/10.1371/JOURNAL.PONE.0147596>
1393 Casadevall, G., Casadevall, J., Duran, C., Osuna, S., 2024. The shortest path method (SPM)
1394 webserver for computational enzyme design. *Protein Eng Des Sel* 37, gzae005.
1395 <https://doi.org/10.1093/protein/gzae005>
1396 Casadevall, G., Duran, C., Osuna, S., 2023. AlphaFold2 and Deep Learning for Elucidating
1397 Enzyme Conformational Flexibility and Its Application for Design. *JACS Au* 3, 1554–
1398 1562. <https://doi.org/10.1021/jacsau.3c00188>
1399 Case, D.A., Aktulga, H.M., Belfon, K., Cerutti, D.S., Cisneros, G.A., Cruzeiro, V.W.D.,
1400 Forouzesh, N., Giese, T.J., Götz, A.W., Gohlke, H., Izadi, S., Kasavajhala, K., Kaymak,
1401 M.C., King, E., Kurtzman, T., Lee, T.S., Li, P., Liu, J., Luchko, T., Luo, R.,
1402 Manathunga, M., Machado, M.R., Nguyen, H.M., O’Hearn, K.A., Onufriev, A. V., Pan,
1403 F., Pantano, S., Qi, R., Rahnamoun, A., Rishch, A., Schott-Verdugo, S., Shajan, A.,
1404 Swails, J., Wang, J., Wei, H., Wu, X., Wu, Y., Zhang, S., Zhao, S., Zhu, Q., Cheatham,
1405 T.E., Roe, D.R., Roitberg, A., Simmerling, C., York, D.M., Nagan, M.C., Merz, K.M.,
1406 2023. AmberTools. *J Chem Inf Model* 63, 6183–6191.
1407 https://doi.org/10.1021/ACS.JCIM.3C01153/ASSET/IMAGES/LARGE/CI3C01153_00
1408 02.JPEG
1409 Castelli, M., Marchetti, F., Osuna, S., F. Oliveira, A.S., Mulholland, A.J., Serapian, S.A.,
1410 Colombo, G., 2024. Decrypting Allosterity in Membrane-Bound K-Ras4B Using
1411 Complementary In Silico Approaches Based on Unbiased Molecular Dynamics
1412 Simulations. *J. Am. Chem. Soc.* 146, 901–919. <https://doi.org/10.1021/jacs.3c11396>
1413 Chen, D., Hartout, P., Pellizzoni, P., Oliver, C., Borgwardt, K., 2024. Endowing Protein
1414 Language Models with Structural Knowledge.
1415 Cheng, J., Randall, A.Z., Sweredoski, M.J., Baldi, P., 2005. SCRATCH: a protein structure
1416 and structural feature prediction server. *Nucleic Acids Res* 33.
1417 <https://doi.org/10.1093/NAR/GKI396>
1418 Cherry, J.R., Fidantsef, A.L., 2003. Directed evolution of industrial enzymes: an update. *Curr*
1419 *Opin Biotechnol* 14, 438–443. [https://doi.org/10.1016/S0958-1669\(03\)00099-5](https://doi.org/10.1016/S0958-1669(03)00099-5)
1420 Cherry, J.R., Lamsa, M.H., Schneider, P., Vind, J., Svendsen, A., Jones, A., Pedersen, A.H.,
1421 1999. Directed evolution of a fungal peroxidase. *Nature Biotechnology* 17:4 17,
1422 379–384. <https://doi.org/10.1038/7939>
1423 Chodera, J.D., Noé, F., 2014. Markov state models of biomolecular conformational
1424 dynamics. *Curr Opin Struct Biol, Theory and simulation / Macromolecular machines* 25,
1425 135–144. <https://doi.org/10.1016/j.sbi.2014.04.002>
1426 Cock, P.J.A., Antao, T., Chang, J.T., Chapman, B.A., Cox, C.J., Dalke, A., Friedberg, I.,
1427 Hamelryck, T., Kauff, F., Wilczynski, B., De Hoon, M.J.L., 2009. Biopython: freely
1428 available Python tools for computational molecular biology and bioinformatics.
1429 *Bioinformatics* 25, 1422–1423. <https://doi.org/10.1093/BIOINFORMATICS/BTP163>

1430 Corbella, M., Pinto, G.P., Kamerlin, S.C.L., 2023. Loop dynamics and the evolution of
1431 enzyme activity. *Nat Rev Chem* 7, 536–547. <https://doi.org/10.1038/s41570-023-00495->
1432 [w](https://doi.org/10.1038/s41570-023-00495-w)

1433 Corso, G., Deng, A., Fry, B., Polizzi, N., Barzilay, R., Jaakkola, T., 2024. Deep Confident
1434 Steps to New Pockets: Strategies for Docking Generalization.

1435 Crean, R.M., Biler, M., Van Der Kamp, M.W., Hengge, A.C., Kamerlin, S.C.L., 2021. Loop
1436 Dynamics and Enzyme Catalysis in Protein Tyrosine Phosphatases. *J Am Chem Soc*
1437 143, 3830–3845.
1438 https://doi.org/10.1021/JACS.0C11806/ASSET/IMAGES/LARGE/JA0C11806_0009.JPEG
1439 EG

1440 Curado-Carballada, C., Feixas, F., Osuna, S., 2019. Molecular Dynamics Simulations on
1441 *Aspergillus niger* Monoamine Oxidase: Conformational Dynamics and Inter-monomer
1442 Communication Essential for Its Efficient Catalysis. *Adv Synth Catal* 361, 2718–2726.
1443 <https://doi.org/10.1002/ADSC.201900158>

1444 Davis, I.W., Baker, D., 2009. RosettaLigand docking with full ligand and receptor flexibility.
1445 *J Mol Biol* 385, 381–392. <https://doi.org/10.1016/J.JMB.2008.11.010>

1446 Dawson, N.L., Lewis, T.E., Das, S., Lees, J.G., Lee, D., Ashford, P., Orengo, C.A., Sillitoe,
1447 I., 2019. CATH protein domain classification (version 4.2) [WWW Document].
1448 University College London. <https://doi.org/https://doi.org/10.5522/04/7937330.v1>

1449 Dawson, N.L., Lewis, T.E., Das, S., Lees, J.G., Lee, D., Ashford, P., Orengo, C.A., Sillitoe,
1450 I., 2017. CATH: An expanded resource to predict protein function through structure and
1451 sequence. *Nucleic Acids Res* 45, D289–D295. <https://doi.org/10.1093/NAR/GKW1098>

1452 Desaphy, J., Raimbaud, E., Ducrot, P., Rognan, D., 2013. Encoding protein-ligand interaction
1453 patterns in fingerprints and graphs. *J Chem Inf Model* 53, 623–637.
1454 https://doi.org/10.1021/CI300566N/SUPPL_FILE/CI300566N_SI_001.PDF

1455 Detlefsen, N.S., Hauberg, S., Boomsma, W., 2022. Learning meaningful representations of
1456 protein sequences. *Nat Commun* 13, 1914.

1457 Devine, P.N., Howard, R.M., Kumar, R., Thompson, M.P., Truppo, M.D., Turner, N.J., 2018.
1458 Extending the application of biocatalysis to meet the challenges of drug development.
1459 *Nature Reviews Chemistry* 2018 2:12 2, 409–421. <https://doi.org/10.1038/s41570-018->
1460 [0055-1](https://doi.org/10.1038/s41570-018-0055-1)

1461 Devlin, J., Chang, M.-W., Lee, K., Toutanova, K., 2018. Bert: Pre-training of deep
1462 bidirectional transformers for language understanding. arXiv preprint arXiv:1810.04805.

1463 Ding, X., Zou, Z., Brooks III, C.L., 2019. Deciphering protein evolution and fitness
1464 landscapes with latent space models. *Nat Commun* 10, 5644.

1465 d’Oelsnitz, S., Diaz, D.J., Kim, W., Acosta, D.J., Dangerfield, T.L., Schechter, M.W., Minus,
1466 M.B., Howard, J.R., Do, H., Loy, J.M., Alper, H.S., Zhang, Y.J., Ellington, A.D., 2024.
1467 Biosensor and machine learning-aided engineering of an amaryllidaceae enzyme. *Nature*
1468 *Communications* 2024 15:1 15, 1–14. <https://doi.org/10.1038/s41467-024-46356-y>

1469 Eberhardt, J., Santos-Martins, D., Tillack, A.F., Forli, S., 2021. AutoDock Vina 1.2.0: New
1470 Docking Methods, Expanded Force Field, and Python Bindings. *J Chem Inf Model* 61,
1471 3891–3898.
1472 https://doi.org/10.1021/ACS.JCIM.1C00203/SUPPL_FILE/CI1C00203_SI_002.ZIP

1473 Elabd, H., Bromberg, Y., Hoarfrost, A., Lenz, T., Franke, A., Wendorff, M., 2020. Amino
1474 acid encoding for deep learning applications. *BMC Bioinformatics* 21, 1–14.
1475 <https://doi.org/10.1186/S12859-020-03546-X/FIGURES/4>

1476 Elia Venanzi, N.A., Basciu, A., Vargiu, A.V., Kiparissides, A., Dalby, P.A., Dikicioglu, D.,
1477 2024. Machine Learning Integrating Protein Structure, Sequence, and Dynamics to
1478 Predict the Enzyme Activity of Bovine Enterokinase Variants. *J. Chem. Inf. Model.*
1479 <https://doi.org/10.1021/acs.jcim.3c00999>

1480 Elnaggar, A., Heinzinger, M., Dallago, C., Rehawi, G., Wang, Y., Jones, L., Gibbs, T., Feher,
1481 T., Angerer, C., Steinegger, M., others, 2021. Prottrans: Toward understanding the
1482 language of life through self-supervised learning. *IEEE Trans Pattern Anal Mach Intell*
1483 44, 7112–7127.

1484 Fasoulis, R., Paliouras, G., Kavraki, L.E., 2021. Graph representation learning for structural
1485 proteomics. *Emerg Top Life Sci* 5, 789. <https://doi.org/10.1042/ETLS20210225>

1486 Feng, Y., Gong, C., Zhu, J., Liu, G., Tang, Y., Li, W., 2023. Prediction of Sites of
1487 Metabolism of CYP3A4 Substrates Utilizing Docking-Derived Geometric Features. *J*
1488 *Chem Inf Model* 63, 4158–4169.
1489 https://doi.org/10.1021/ACS.JCIM.3C00549/SUPPL_FILE/CI3C00549_SI_002.XLSX

1490 Ferruz, N., Höcker, B., 2022. Controllable protein design with language models. *Nature*
1491 *Machine Intelligence* 2022 4:6 4, 521–532. <https://doi.org/10.1038/s42256-022-00499-z>

1492 Ferruz, N., Schmidt, S., Höcker, B., 2022. ProtGPT2 is a deep unsupervised language model
1493 for protein design. *Nat Commun* 13, 4348.

1494 Folkman, L., Stantic, B., Sattar, A., Zhou, Y., 2016. EASE-MM: Sequence-Based Prediction
1495 of Mutation-Induced Stability Changes with Feature-Based Multiple Models. *J Mol Biol*
1496 428, 1394–1405. <https://doi.org/10.1016/J.JMB.2016.01.012>

1497 Fox, R., 2005. Directed molecular evolution by machine learning and the influence of
1498 nonlinear interactions. *J Theor Biol* 234, 187–199.
1499 <https://doi.org/10.1016/J.JTBI.2004.11.031>

1500 Fraczkiewicz, R., Braun, W., 1998. Exact and efficient analytical calculation of the accessible
1501 surface areas and their gradients for macromolecules. *J Comput Chem* 19, 319–333.
1502 [https://doi.org/10.1002/\(sici\)1096-987x\(199802\)19:3<319::aid-jcc6>3.0.co](https://doi.org/10.1002/(sici)1096-987x(199802)19:3<319::aid-jcc6>3.0.co)

1503 France, S.P., Hepworth, L.J., Turner, N.J., Flitsch, S.L., 2017. Constructing Biocatalytic
1504 Cascades: In Vitro and in Vivo Approaches to de Novo Multi-Enzyme Pathways. *ACS*
1505 *Catal* 7, 710–724.
1506 <https://doi.org/10.1021/ACSCATAL.6B02979/ASSET/IMAGES/LARGE/CS-2016->
1507 [02979U_0018.JPEG](https://doi.org/10.1021/ACSCATAL.6B02979/ASSET/IMAGES/LARGE/CS-2016-02979U_0018.JPEG)

1508 Frazer, J., Notin, P., Dias, M., Gomez, A., Min, J.K., Brock, K., Gal, Y., Marks, D.S., 2021.
1509 Disease variant prediction with deep generative models of evolutionary data. *Nature*
1510 599, 91–95.

1511 Gainza, P., Sverrisson, F., Monti, F., Rodolà, E., Boscaini, D., Bronstein, M.M., Correia,
1512 B.E., 2019. Deciphering interaction fingerprints from protein molecular surfaces using
1513 geometric deep learning. *Nature Methods* 2019 17:2 17, 184–192.
1514 <https://doi.org/10.1038/s41592-019-0666-6>

1515 Galanie, S., Entwistle, D., Lalonde, J., 2020. Engineering biosynthetic enzymes for industrial
1516 natural product synthesis. *Nat Prod Rep* 37, 1122–1143.
1517 <https://doi.org/10.1039/C9NP00071B>

1518 Galdadas, I., Qu, S., Oliveira, A.S.F., Olehnovics, E., Mack, A.R., Mojica, M.F., Agarwal,
1519 P.K., Tooke, C.L., Gervasio, F.L., Spencer, J., Bonomo, R.A., Mulholland, A.J., Haider,
1520 S., 2021. Allosteric communication in class A β -lactamases occurs via cooperative
1521 coupling of loop dynamics. *Elife* 10.

1522 Gandomkar, S., Źądło-Dobrowolska, A., Kroutil, W., 2019. Extending Designed Linear
1523 Biocatalytic Cascades for Organic Synthesis. *ChemCatChem* 11, 225–243.
1524 <https://doi.org/10.1002/CCTC.201801063>

1525 Gergel, S., Soler, J., Klein, A., Schülke, K.H., Hauer, B., Garcia-Borràs, M., Hammer, S.C.,
1526 2023. Engineered cytochrome P450 for direct arylalkene-to-ketone oxidation via highly
1527 reactive carbocation intermediates. *Nature Catalysis* 2023 6:7 6, 606–617.
1528 <https://doi.org/10.1038/s41929-023-00979-4>

1529 Ghorbani, M., Prasad, S., Klauda, J.B., Brooks, B.R., 2022. GraphVAMPNet, using graph
1530 neural networks and variational approach to Markov processes for dynamical modeling
1531 of biomolecules. *J Chem Phys* 156, 184103. <https://doi.org/10.1063/5.0085607>
1532 Giessel, A., Dousis, A., Ravichandran, K., Smith, K., Sur, S., McFadyen, I., Zheng, W.,
1533 Licht, S., 2022. Therapeutic enzyme engineering using a generative neural network. *Sci*
1534 *Rep* 12, 1536.
1535 Giver, L., Gershenson, A., Freskgard, P.O., Arnold, F.H., 1998. Directed evolution of a
1536 thermostable esterase. *Proceedings of the National Academy of Sciences* 95, 12809–
1537 12813. <https://doi.org/10.1073/PNAS.95.22.12809>
1538 Gligorijević, V., Renfrew, P.D., Kosciolk, T., Leman, J.K., Berenberg, D., Vatanen, T.,
1539 Chandler, C., Taylor, B.C., Fisk, I.M., Vlamakis, H., Xavier, R.J., Knight, R., Cho, K.,
1540 Bonneau, R., 2021. Structure-based protein function prediction using graph
1541 convolutional networks. *Nature Communications* 2021 12:1 12, 1–14.
1542 <https://doi.org/10.1038/s41467-021-23303-9>
1543 Goblirsch, B.R., Jensen, M.R., Mohamed, F.A., Wackett, L.P., Wilmot, C.M., 2016.
1544 Substrate trapping in crystals of the thiolase olea identifies three channels that enable
1545 long chain olefin biosynthesis. *Journal of Biological Chemistry* 291, 26698–26706.
1546 <https://doi.org/10.1074/JBC.M116.760892>
1547 Goldman, S., Das, R., Yang, K.K., Coley, C.W., 2022. Machine learning modeling of family
1548 wide enzyme-substrate specificity screens. *PLoS Comput Biol* 18, e1009853.
1549 <https://doi.org/10.1371/JOURNAL.PCBI.1009853>
1550 Gordon, S.E., Weber, D.K., Downton, M.T., Wagner, J., Perugini, M.A., 2016. Dynamic
1551 Modelling Reveals ‘Hotspots’ on the Pathway to Enzyme-Substrate Complex
1552 Formation. *PLoS Comput Biol* 12, e1004811.
1553 <https://doi.org/10.1371/journal.pcbi.1004811>
1554 Greenhalgh, J.C., Fahlberg, S.A., Pflieger, B.F., Romero, P.A., 2021. Machine learning-
1555 guided acyl-ACP reductase engineering for improved in vivo fatty alcohol production.
1556 *Nature Communications* 2021 12:1 12, 1–10. [https://doi.org/10.1038/s41467-021-](https://doi.org/10.1038/s41467-021-25831-w)
1557 [25831-w](https://doi.org/10.1038/s41467-021-25831-w)
1558 Hamelryck, T., 2005. An amino acid has two sides: a new 2D measure provides a different
1559 view of solvent exposure. *Proteins* 59, 38–48. <https://doi.org/10.1002/PROT.20379>
1560 Harding-Larsen, D., Madsen, C.D., Teze, D., Kittilä, T., Langhorn, M.R., Gharabli, H.,
1561 Hobusch, M., Otalvaro, F.M., Kirtel, O., Bidart, G.N., Mazurenko, S., Travnik, E.,
1562 Welner, D.H., 2023. GASP: A pan-specific predictor of family 1 glycosyltransferase
1563 specificity enabled by a pipeline for substrate feature generation and large-scale
1564 experimental screening. <https://doi.org/10.26434/CHEMRXIV-2023-PR9CK>
1565 Hauer, B., 2020. Embracing Nature’s Catalysts: A Viewpoint on the Future of Biocatalysis.
1566 *ACS Catal* 10, 8418–8427.
1567 [https://doi.org/10.1021/ACSCATAL.0C01708/ASSET/IMAGES/LARGE/CS0C01708_](https://doi.org/10.1021/ACSCATAL.0C01708/ASSET/IMAGES/LARGE/CS0C01708_0003.JPG)
1568 [0003.JPG](https://doi.org/10.1021/ACSCATAL.0C01708/ASSET/IMAGES/LARGE/CS0C01708_0003.JPG)
1569 Hawkins-Hooker, A., Depardieu, F., Baur, S., Couairon, G., Chen, A., Bikard, D., 2021.
1570 Generating functional protein variants with variational autoencoders. *PLoS Comput Biol*
1571 17, e1008736.
1572 Heath, R.S., Ruscoe, R.E., Turner, N.J., 2022. The beauty of biocatalysis: sustainable
1573 synthesis of ingredients in cosmetics. *Nat Prod Rep* 39, 335–388.
1574 <https://doi.org/10.1039/D1NP00027F>
1575 Heckmann, D., Campeau, A., Lloyd, C.J., Phaneuf, P. V., Hefner, Y., Carrillo-Terrazas, M.,
1576 Feist, A.M., Gonzalez, D.J., Palsson, B.O., 2020. Kinetic profiling of metabolic
1577 specialists demonstrates stability and consistency of in vivo enzyme turnover numbers.
1578 *Proc Natl Acad Sci U S A* 117, 23182–23190.

1579 https://doi.org/10.1073/PNAS.2001562117/SUPPL_FILE/PNAS.2001562117.SD01.XL
1580 SX

1581 Heckmann, D., Lloyd, C.J., Mih, N., Ha, Y., Zielinski, D.C., Haiman, Z.B., Desouki, A.A.,
1582 Lercher, M.J., Palsson, B.O., 2018. Machine learning applied to enzyme turnover
1583 numbers reveals protein structural correlates and improves metabolic models. *Nature*
1584 *Communications* 2018 9:1 9, 1–10. <https://doi.org/10.1038/s41467-018-07652-6>

1585 Heffernan, R., Yang, Y., Paliwal, K., Zhou, Y., 2017. Capturing non-local interactions by
1586 long short-term memory bidirectional recurrent neural networks for improving
1587 prediction of protein secondary structure, backbone angles, contact numbers and solvent
1588 accessibility. *Bioinformatics* 33, 2842–2849.
1589 <https://doi.org/10.1093/BIOINFORMATICS/BTX218>

1590 Heinzinger, Michael, Weissenow, Konstantin, Gomez Sanchez, Joaquin, Henkel, Adrian,
1591 Steinegger, Martin, Rost, B., Heinzinger, M, Weissenow, K, Gomez Sanchez, J, Henkel,
1592 A, Steinegger, M, Probst, R., 2023. ProST5: Bilingual Language Model for Protein
1593 Sequence and Structure. *bioRxiv* 2023.07.23.550085.
1594 <https://doi.org/10.1101/2023.07.23.550085>

1595 Hellberg, S., Sjöström, M., Skagerberg, B., Wold, S., 1987. Peptide Quantitative Structure-
1596 Activity Relationships, a Multivariate Approach. *J Med Chem* 30, 1126–1135.
1597 https://doi.org/10.1021/JM00390A003/SUPPL_FILE/JM00390A003_SI_001.PDF

1598 Henikoff, S., Henikoff, J.G., 1992. Amino acid substitution matrices from protein blocks.
1599 *Proceedings of the National Academy of Sciences* 89, 10915–10919.
1600 <https://doi.org/10.1073/PNAS.89.22.10915>

1601 Henzler-Wildman, K., Kern, D., 2007. Dynamic personalities of proteins. *Nature* 450.

1602 Hoffbauer, T., Strodel, B., 2024. TransMEP: Transfer learning on large protein language
1603 models to predict mutation effects of proteins from a small known dataset. *bioRxiv*
1604 2021–2024.

1605 Hon, J., Borko, S., Stourac, J., Prokop, Z., Zendulka, J., Bednar, D., Martinek, T.,
1606 Damborsky, J., 2020. EnzymeMiner: automated mining of soluble enzymes with diverse
1607 structures, catalytic properties and stabilities. *Nucleic Acids Res* 48, W104–W109.
1608 <https://doi.org/10.1093/NAR/GKAA372>

1609 Hou, X., Wang, Yu, Bu, D., Wang, Yaojun, Sun, S., 2023. EMNGly: predicting N-linked
1610 glycosylation sites using the language models for feature extraction. *Bioinformatics* 39.
1611 <https://doi.org/10.1093/BIOINFORMATICS/BTAD650>

1612 Hsu, C., Nisonoff, H., Fannjiang, C., Listgarten, J., 2022. Learning protein fitness models
1613 from evolutionary and assay-labeled data. *Nat Biotechnol* 40, 1114–1122.
1614 <https://doi.org/10.1038/S41587-021-01146-5>

1615 Huang, T.W., Zaretski, J., Bergeron, C., Bennett, K.P., Breneman, C.M., 2013. DR-Predictor:
1616 Incorporating flexible docking with specialized electronic reactivity and machine
1617 learning techniques to predict CYP-mediated sites of metabolism. *J Chem Inf Model* 53,
1618 3352–3366. https://doi.org/10.1021/CI4004688/SUPPL_FILE/CI4004688_SI_001.ZIP

1619 Huffman, M.A., Fryszkowska, A., Alvizo, O., Borra-Garske, M., Campos, K.R., Canada,
1620 K.A., Devine, P.N., Duan, D., Forstater, J.H., Grosser, S.T., Halsey, H.M., Hughes, G.J.,
1621 Jo, J., Joyce, L.A., Kolev, J.N., Liang, J., Maloney, K.M., Mann, B.F., Marshall, N.M.,
1622 McLaughlin, M., Moore, J.C., Murphy, G.S., Nawrat, C.C., Nazor, J., Novick, S., Patel,
1623 N.R., Rodriguez-Granillo, A., Robaire, S.A., Sherer, E.C., Truppo, M.D., Whittaker,
1624 A.M., Verma, D., Xiao, L., Xu, Y., Yang, H., 2019. Design of an in vitro biocatalytic
1625 cascade for the manufacture of islatravir. *Science* (1979) 366, 1255–1259.
1626 [https://doi.org/10.1126/SCIENCE.AAY8484/SUPPL_FILE/AAY8484-HUFFMAN-](https://doi.org/10.1126/SCIENCE.AAY8484/SUPPL_FILE/AAY8484-HUFFMAN-SM.PDF)
1627 [SM.PDF](https://doi.org/10.1126/SCIENCE.AAY8484/SUPPL_FILE/AAY8484-HUFFMAN-SM.PDF)

1628 Ibtihaz, N., Kagaya, Y., Kihara, D., 2023. Domain-PFP allows protein function prediction
1629 using function-aware domain embedding representations. *Communications Biology*
1630 2023 6:1 6, 1–14. <https://doi.org/10.1038/s42003-023-05476-9>
1631 Iqbal, S., Ge, F., Li, F., Akutsu, T., Zheng, Y., Gasser, R.B., Yu, D.J., Webb, G.I., Song, J.,
1632 2022. PROST: AlphaFold2-aware Sequence-Based Predictor to Estimate Protein
1633 Stability Changes upon Missense Mutations. *J Chem Inf Model*.
1634 https://doi.org/10.1021/ACS.JCIM.2C00799/SUPPL_FILE/CI2C00799_SI_001.PDF
1635 Isert, C., Atz, K., Schneider, G., 2023. Structure-based drug design with geometric deep
1636 learning. *Curr Opin Struct Biol* 79, 102548. <https://doi.org/10.1016/J.SBI.2023.102548>
1637 Iuchi, H., Matsutani, T., Yamada, K., Iwano, N., Sumi, S., Hosoda, S., Zhao, S., Fukunaga,
1638 T., Hamada, M., 2021. Representation learning applications in biological sequence
1639 analysis. *Comput Struct Biotechnol J* 19, 3198–3208.
1640 Jing, B., Berger, B., Jaakkola, T., 2024. AlphaFold Meets Flow Matching for Generating
1641 Protein Ensembles.
1642 Jonsson, J., Eriksson, L., Hellberg, S., Sjöström, M., Wold, S., 1989. Multivariate
1643 Parametrization of 55 Coded and Non-Coded Amino Acids. *Quantitative Structure-*
1644 *Activity Relationships* 8, 204–209. <https://doi.org/10.1002/QSAR.19890080303>
1645 Jumper, J., Evans, R., Pritzel, A., Green, T., Figurnov, M., Ronneberger, O.,
1646 Tunyasuvunakool, K., Bates, R., Židek, A., Potapenko, A., Bridgland, A., Meyer, C.,
1647 Kohl, S.A.A., Ballard, A.J., Cowie, A., Romera-Paredes, B., Nikolov, S., Jain, R., Adler,
1648 J., Back, T., Petersen, S., Reiman, D., Clancy, E., Zielinski, M., Steinegger, M.,
1649 Pacholska, M., Berghammer, T., Bodenstein, S., Silver, D., Vinyals, O., Senior, A.W.,
1650 Kavukcuoglu, K., Kohli, P., Hassabis, D., 2021. Highly accurate protein structure
1651 prediction with AlphaFold. *Nature* 2021 596:7873 596, 583–589.
1652 <https://doi.org/10.1038/s41586-021-03819-2>
1653 Kamerlin, S.C.L., Warshel, A., 2010. At the dawn of the 21st century: Is dynamics the
1654 missing link for understanding enzyme catalysis? *Proteins: Structure, Function, and*
1655 *Bioinformatics* 78, 1339–1375. <https://doi.org/10.1002/prot.22654>
1656 Kanakala, G.C., Aggarwal, R., Nayar, D., Priyakumar, U.D., 2022. Latent Biases in Machine
1657 Learning Models for Predicting Binding Affinities Using Popular Data Sets. *ACS*
1658 *Omega*.
1659 https://doi.org/10.1021/ACSOMEGA.2C06781/ASSET/IMAGES/LARGE/AO2C06781_0004.JPEG
1660
1661 Karlov, D.S., Long, S.L., Zeng, X., Xu, F., Lal, K., Cao, L., Hayoun, K., Lin, J., Joyce, S.A.,
1662 Tikhonova, I.G., 2023. Characterization of the mechanism of bile salt hydrolase
1663 substrate specificity by experimental and computational analyses. *Structure* 31, 629-
1664 638.e5. <https://doi.org/10.1016/J.STR.2023.02.014>
1665 Kawashima, S., Kanehisa, M., 2000. AAindex: Amino Acid index database. *Nucleic Acids*
1666 *Res* 28, 374–374. <https://doi.org/10.1093/NAR/28.1.374>
1667 Kazan, I.C., Mills, J.H., Ozkan, S.B., 2023. Allosteric regulatory control in dihydrofolate
1668 reductase is revealed by dynamic asymmetry. *Protein Science* 32, e4700.
1669 <https://doi.org/10.1002/pro.4700>
1670 Khan, N.R., Rathod, V.K., 2015. Enzyme catalyzed synthesis of cosmetic esters and its
1671 intensification: A review. *Process Biochemistry* 50, 1793–1806.
1672 <https://doi.org/10.1016/J.PROCBIO.2015.07.014>
1673 Kim, A.K., Porter, L.L., 2021. Functional and Regulatory Roles of Fold-Switching Proteins.
1674 *Structure* 29, 6–14. <https://doi.org/10.1016/J.STR.2020.10.006>
1675 Kingma, D.P., Welling, M., 2013. Auto-encoding variational bayes. arXiv preprint
1676 arXiv:1312.6114.

1677 Kirk, O., Borchert, T.V., Fuglsang, C.C., 2002. Industrial enzyme applications. *Curr Opin*
1678 *Biotechnol* 13, 345–351. [https://doi.org/10.1016/S0958-1669\(02\)00328-2](https://doi.org/10.1016/S0958-1669(02)00328-2)

1679 Kohout, P., Vasina, M., Majerova, M., Novakova, V., Damborsky, J., Bednar, D., Marek, M.,
1680 Prokop, Z., Mazurenko, S., 2023. Design of Enzymes for Biocatalysis, Bioremediation,
1681 and Biosensing using Variational Autoencoder-Generated Latent Spaces.

1682 Konovalov, K.A., Unarta, I.C., Cao, S., Goonetilleke, E.C., Huang, X., 2021. Markov State
1683 Models to Study the Functional Dynamics of Proteins in the Wake of Machine Learning.
1684 *JACS Au* 1, 1330–1341. <https://doi.org/10.1021/jacsau.1c00254>

1685 Kouba, P., Kohout, P., Haddadi, F., Bushuiev, A., Samusevich, R., Sedlar, J., Damborsky, J.,
1686 Pluskal, T., Sivic, J., Mazurenko, S., 2023. Machine Learning-Guided Protein
1687 Engineering. *ACS Catal* 13, 13863–13895.
1688 <https://doi.org/10.1021/ACSCATAL.3C02743>

1689 Kroll, A., Lercher, M.J., 2023. Machine learning models for the prediction of enzyme
1690 properties should be tested on proteins not used for model training. *bioRxiv*
1691 2023.02.06.526991. <https://doi.org/10.1101/2023.02.06.526991>

1692 Kroll, A., Ranjan, S., Engqvist, M.K.M., Lercher, M.J., 2023a. A general model to predict
1693 small molecule substrates of enzymes based on machine and deep learning. *Nature*
1694 *Communications* 2023 14:1 14, 1–13. <https://doi.org/10.1038/s41467-023-38347-2>

1695 Kroll, A., Rousset, Y., Hu, X.P., Liebrand, N.A., Lercher, M.J., 2023b. Turnover number
1696 predictions for kinetically uncharacterized enzymes using machine and deep learning.
1697 *Nature Communications* 2023 14:1 14, 1–14. [https://doi.org/10.1038/s41467-023-](https://doi.org/10.1038/s41467-023-39840-4)
1698 39840-4

1699 Kunka, A., Marques, S.M., Havlasek, M., Vasina, M., Velatova, N., Cengelova, L., Kovar,
1700 D., Damborsky, J., Marek, M., Bednar, D., Prokop, Z., 2023. Advancing Enzyme's
1701 Stability and Catalytic Efficiency through Synergy of Force-Field Calculations,
1702 Evolutionary Analysis, and Machine Learning. *ACS Catal* 13, 12506–12518.
1703 https://doi.org/10.1021/ACSCATAL.3C02575/SUPPL_FILE/CS3C02575_SI_005.XLS
1704 X

1705 Lane, T.J., 2023. Protein structure prediction has reached the single-structure frontier. *Nat*
1706 *Methods* 20, 170–173. <https://doi.org/10.1038/s41592-022-01760-4>

1707 Le Guilloux, V., Schmidtke, P., Tuffery, P., 2009. Fpocket: An open source platform for
1708 ligand pocket detection. *BMC Bioinformatics* 10, 1–11. [https://doi.org/10.1186/1471-](https://doi.org/10.1186/1471-2105-10-168/TABLES/1)
1709 2105-10-168/TABLES/1

1710 Lee, B., Richards, F.M., 1971. The interpretation of protein structures: Estimation of static
1711 accessibility. *J Mol Biol* 55, 379-IN4. [https://doi.org/10.1016/0022-2836\(71\)90324-X](https://doi.org/10.1016/0022-2836(71)90324-X)

1712 Leidner, F., Kurt Yilmaz, N., Schiffer, C.A., 2019. Target-Specific Prediction of Ligand
1713 Affinity with Structure-Based Interaction Fingerprints. *J Chem Inf Model* 59, 3679–
1714 3691.
1715 https://doi.org/10.1021/ACS.JCIM.9B00457/SUPPL_FILE/CI9B00457_SI_001.PDF

1716 Li, B., Yang, Y.T., Capra, J.A., Gerstein, M.B., 2020. Predicting changes in protein
1717 thermodynamic stability upon point mutation with deep 3D convolutional neural
1718 networks. *PLoS Comput Biol* 16. <https://doi.org/10.1371/JOURNAL.PCBI.1008291>

1719 Li, F., Yuan, L., Lu, H., Li, G., Chen, Y., Engqvist, M.K.M., Kerkhoven, E.J., Nielsen, J.,
1720 2022. Deep learning-based kcat prediction enables improved enzyme-constrained model
1721 reconstruction. *Nature Catalysis* 2022 5:8 5, 662–672. [https://doi.org/10.1038/s41929-](https://doi.org/10.1038/s41929-022-00798-z)
1722 022-00798-z

1723 Li, G., Qin, Y., Fontaine, N.T., Ng Fuk Chong, M., Maria-Solano, M.A., Feixas, F., Cadet,
1724 X.F., Pandjaitan, R., Garcia-Borràs, M., Cadet, F., Reetz, M.T., 2021. Machine Learning
1725 Enables Selection of Epistatic Enzyme Mutants for Stability Against Unfolding and

1726 Detrimental Aggregation. *Chembiochem* 22, 904–914.
1727 <https://doi.org/10.1002/CBIC.202000612>

1728 Li, J., Guan, X., Zhang, O., Sun, K., Wang, Y., Bagni, D., Head-Gordon, T., Pitzer, †, 2023.
1729 Leak Proof PDBBind: A Reorganized Dataset of Protein-Ligand Complexes for More
1730 Generalizable Binding Affinity Prediction. *ArXiv*.

1731 Li, M., Wang, H., Yang, Z., Zhang, L., Zhu, Y., 2023. DeepTM: A deep learning algorithm
1732 for prediction of melting temperature of thermophilic proteins directly from sequences.
1733 *Comput Struct Biotechnol J* 21, 5544–5560. <https://doi.org/10.1016/j.csbj.2023.11.006>

1734 Lin, Z., Akin, H., Rao, R., Hie, B., Zhu, Z., Lu, W., Smetanin, N., Verkuil, R., Kabeli, O.,
1735 Shmueli, Y., dos Santos Costa, A., Fazel-Zarandi, M., Sercu, T., Candido, S., Rives, A.,
1736 2023. Evolutionary-scale prediction of atomic-level protein structure with a language
1737 model. *Science (1979)* 379, 1123–1130.
1738 https://doi.org/10.1126/SCIENCE.ADE2574/SUPPL_FILE/SCIENCE.ADE2574_SM.PDF
1739 DF

1740 Livesey, B.J., Marsh, J.A., 2023. Updated benchmarking of variant effect predictors using
1741 deep mutational scanning. *Mol Syst Biol* e11474.

1742 Lu, C., Lubin, J.H., Sarma, V. V., Stentz, S.Z., Wang, G., Wang, S., Khare, S.D., 2023.
1743 Prediction and design of protease enzyme specificity using a structure-aware graph
1744 convolutional network. *Proc Natl Acad Sci U S A* 120, e2303590120.
1745 https://doi.org/10.1073/PNAS.2303590120/SUPPL_FILE/PNAS.2303590120.SD07.XLSX
1746 SX

1747 Ma, E.J., Siirola, E., Moore, C., Kummer, A., Stoeckli, M., Faller, M., Bouquet, C.,
1748 Eggimann, F., Ligibel, M., Huynh, D., Cutler, G., Siegrist, L., Lewis, R.A., Acker, A.C.,
1749 Freund, E., Koch, E., Vogel, M., Schlingensiepen, H., Oakeley, E.J., Snajdrova, R.,
1750 2021. Machine-Directed Evolution of an Imine Reductase for Activity and
1751 Stereoselectivity. *ACS Catal* 11, 12433–12445.
1752 https://doi.org/10.1021/ACSCATAL.1C02786/SUPPL_FILE/CS1C02786_SI_003.CSV

1753 Mansoor, S., Baek, M., Park, H., Lee, G.R., Baker, D., 2023. Protein Ensemble Generation
1754 through Variational Autoencoder Latent Space Sampling. *bioRxiv*.
1755 <https://doi.org/10.1101/2023.08.01.551540>

1756 Mardt, A., Pasquali, L., Wu, H., Noé, F., 2018. VAMPnets for deep learning of molecular
1757 kinetics. *Nat Commun* 9, 5. <https://doi.org/10.1038/s41467-017-02388-1>

1758 Maria-Solano, M.A., Kinateder, T., Iglesias-Fernández, J., Sterner, R., Osuna, S., 2021. In
1759 Silico identification and experimental validation of distal activity-enhancing mutations
1760 in tryptophan synthase. *ACS Catal* 11, 13733–13743.
1761 https://doi.org/10.1021/ACSCATAL.1C03950/SUPPL_FILE/CS1C03950_SI_001.PDF

1762 Markus, B., Christian C, G., Andreas, K., Arkadij, K., Stefan, L., Gustav, O., Elina, S.,
1763 Radka, S., 2023. Accelerating Biocatalysis Discovery with Machine Learning: A
1764 Paradigm Shift in Enzyme Engineering, Discovery, and Design. *ACS Catal* 13, 14454–
1765 14469. <https://doi.org/10.1021/ACSCATAL.3C03417>

1766 Mastropietro, A., Pasculli, G., Bajorath, J., 2023. Learning characteristics of graph neural
1767 networks predicting protein–ligand affinities. *Nature Machine Intelligence* 2023 5:12 5,
1768 1427–1436. <https://doi.org/10.1038/s42256-023-00756-9>

1769 Mazurenko, S., Prokop, Z., Damborsky, J., 2020. Machine Learning in Enzyme Engineering.
1770 *ACS Catal* 10, 1210–1223.
1771 https://doi.org/10.1021/ACSCATAL.9B04321/ASSET/IMAGES/LARGE/CS9B04321_0004.JPEG
1772 0004.JPEG

1773 McGibbon, R.T., Beauchamp, K.A., Harrigan, M.P., Klein, C., Swails, J.M., Hernández,
1774 C.X., Schwantes, C.R., Wang, L.P., Lane, T.J., Pande, V.S., 2015. MDTraj: A Modern

1775 Open Library for the Analysis of Molecular Dynamics Trajectories. *Biophys J* 109,
1776 1528. <https://doi.org/10.1016/J.BPJ.2015.08.015>

1777 Mei, H., Liao, Z.H., Zhou, Y., Li, S.Z., 2005. A new set of amino acid descriptors and its
1778 application in peptide QSARs. *Peptide Science* 80, 775–786.
1779 <https://doi.org/10.1002/BIP.20296>

1780 Meiler, J., Baker, D., 2006. ROSETTALIGAND: Protein–small molecule docking with full
1781 side-chain flexibility. *Proteins: Structure, Function, and Bioinformatics* 65, 538–548.
1782 <https://doi.org/10.1002/PROT.21086>

1783 Meiler, J., Müller, M., Zeidler, A., Schmäschke, F., 2001. Generation and evaluation of
1784 dimension-reduced amino acid parameter representations by artificial neural networks. *J*
1785 *Mol Model* 7, 360–369. <https://doi.org/10.1007/S008940100038/METRICS>

1786 Michael, R., Kæstel-Hansen, J., Groth, P.M., Bartels, S., Salomon, J., Tian, P., Hatzakis,
1787 N.S., Boomsma, W.K., 2023. Assessing the performance of protein regression models.
1788 *bioRxiv* 2023.06.18.545472. <https://doi.org/10.1101/2023.06.18.545472>

1789 Mohanan, N., Montazer, Z., Sharma, P.K., Levin, D.B., 2020. Microbial and Enzymatic
1790 Degradation of Synthetic Plastics. *Front Microbiol* 11, 580709.
1791 <https://doi.org/10.3389/FMICB.2020.580709/BIBTEX>

1792 Morra, G., Potestio, R., Micheletti, C., Colombo, G., 2012. Corresponding Functional
1793 Dynamics across the Hsp90 Chaperone Family: Insights from a Multiscale Analysis of
1794 MD Simulations. *PLoS Comput Biol* 8, e1002433.
1795 <https://doi.org/10.1371/JOURNAL.PCBI.1002433>

1796 Mou, Z., Eakes, J., Cooper, C.J., Foster, C.M., Standaert, R.F., Podar, M., Doktycz, M.J.,
1797 Parks, J.M., 2021. Machine learning-based prediction of enzyme substrate scope:
1798 Application to bacterial nitrilases. *Proteins: Structure, Function, and Bioinformatics* 89,
1799 336–347. <https://doi.org/10.1002/PROT.26019>

1800 Mount, D.W., 2008. Using BLOSUM in sequence alignments. *Cold Spring Harb Protoc* 3.
1801 <https://doi.org/10.1101/PDB.TOP39>

1802 Nazor, J., Liu, J., Huisman, G., 2021. Enzyme evolution for industrial biocatalytic cascades.
1803 *Curr Opin Biotechnol* 69, 182–190. <https://doi.org/10.1016/J.COPBIO.2020.12.013>

1804 Noé, F., Tkatchenko, A., Müller, K.-R., Clementi, C., 2020. Machine Learning for Molecular
1805 Simulation. *Annu Rev Phys Chem* 71, 361–390. <https://doi.org/10.1146/annurev-physchem-042018-052331>

1807 Notin, P., Kollasch, A.W., Ritter, D., Niekerk, L. Van, Paul, S., Spinner, H., Rollins, N.J.,
1808 Shaw, A., Weitzman, R., Frazer, J., Dias, M., Franceschi, D., Orenbuch, R., Gal, Y.,
1809 Marks, D.S., 2023. ProteinGym: Large-Scale Benchmarks for Protein Fitness Prediction
1810 and Design.

1811 Novakovsky, G., Dexter, N., Libbrecht, M.W., Wasserman, W.W., Mostafavi, S., 2022.
1812 Obtaining genetics insights from deep learning via explainable artificial intelligence.
1813 *Nature Reviews Genetics* 2022 24:2 24, 125–137. <https://doi.org/10.1038/s41576-022-00532-2>

1815 Oberg, N., Zallot, R., Gerlt, J.A., 2023. EFI-EST, EFI-GNT, and EFI-CGFP: Enzyme
1816 Function Initiative (EFI) Web Resource for Genomic Enzymology Tools. *J Mol Biol*
1817 435, 168018. <https://doi.org/10.1016/J.JMB.2023.168018>

1818 Oliveira, A.S.F., Ciccotti, G., Haider, S., Mulholland, A.J., 2021. Dynamical nonequilibrium
1819 molecular dynamics reveals the structural basis for allostery and signal propagation in
1820 biomolecular systems. *Eur. Phys. J. B* 94.

1821 Osuna, S., 2021. The challenge of predicting distal active site mutations in computational
1822 enzyme design. *WIREs Computational Molecular Science* 11.
1823 <https://doi.org/10.1002/wcms.1502>

1824 Paik, I., Ngo, P.H.T., Shroff, R., Diaz, D.J., Maranhao, A.C., Walker, D.J.F., Bhadra, S.,
1825 Ellington, A.D., 2023. Improved Bst DNA Polymerase Variants Derived via a Machine
1826 Learning Approach. *Biochemistry* 62, 410–418.
1827 <https://doi.org/10.1021/ACS.BIOCHEM.1C00451>/ASSET/IMAGES/LARGE/BI1C004
1828 51_0006.JPEG

1829 Qiu, Y., Wei, G.W., 2023. Artificial intelligence-aided protein engineering: from topological
1830 data analysis to deep protein language models. *Brief Bioinform* 24, 1–13.
1831 <https://doi.org/10.1093/BIB/BBAD289>

1832 Qu, G., Li, A., Acevedo-Rocha, C.G., Sun, Z., Reetz, M.T., 2020. The Crucial Role of
1833 Methodology Development in Directed Evolution of Selective Enzymes. *Angewandte*
1834 *Chemie International Edition* 59, 13204–13231.
1835 <https://doi.org/10.1002/ANIE.201901491>

1836 Radley, E., Davidson, J., Foster, J., Obexer, R., Bell, E.L., Green, A.P., 2023. Engineering
1837 Enzymes for Environmental Sustainability. *Angewandte Chemie International Edition*
1838 62, e202309305. <https://doi.org/10.1002/ANIE.202309305>

1839 Raimondi, D., Orlando, G., Vranken, W.F., Moreau, Y., 2019. Exploring the limitations of
1840 biophysical propensity scales coupled with machine learning for protein sequence
1841 analysis. *Scientific Reports* 2019 9:1 9, 1–11. <https://doi.org/10.1038/s41598-019-53324-w>

1843 Ran, X., Jiang, Y., Shao, Q., Yang, Z.J., 2023. EnzyKR: a chirality-aware deep learning
1844 model for predicting the outcomes of the hydrolase-catalyzed kinetic resolution. *Chem*
1845 *Sci* 14, 12073–12082. <https://doi.org/10.1039/D3SC02752J>

1846 Rao, R., Meier, J., Sercu, T., Ovchinnikov, S., Rives, A., 2020. Transformer protein language
1847 models are unsupervised structure learners. *Biorxiv* 2012–2020.

1848 Rao, R.M., Liu, J., Verkuil, R., Meier, J., Canny, J., Abbeel, P., Sercu, T., Rives, A., 2021.
1849 MSA Transformer. *PMLR*, pp. 8844–8856.

1850 Raudys, S.J., Jain, A.K., 1991. Small Sample Size Effects in Statistical Pattern Recognition:
1851 Recommendations for Practitioners. *IEEE Trans Pattern Anal Mach Intell* 13, 252–264.
1852 <https://doi.org/10.1109/34.75512>

1853 Reetz, M.T., Qu, G., Sun, Z., 2024. Engineered enzymes for the synthesis of pharmaceuticals
1854 and other high-value products. *Nature Synthesis* 2024 3:1 3, 19–32.
1855 <https://doi.org/10.1038/s44160-023-00417-0>

1856 Renata, H., Wang, Z.J., Arnold, F.H., 2015. Expanding the Enzyme Universe: Accessing
1857 Non-Natural Reactions by Mechanism-Guided Directed Evolution. *Angewandte Chemie*
1858 *International Edition* 54, 3351–3367. <https://doi.org/10.1002/ANIE.201409470>

1859 Richards, F.M., 1977. Areas, volumes, packing and protein structure. *Annu Rev Biophys*
1860 *Bioeng* 6, 151–176. <https://doi.org/10.1146/ANNUREV.BB.06.060177.001055>

1861 Riesselman, A.J., Ingraham, J.B., Marks, D.S., 2018. Deep generative models of genetic
1862 variation capture the effects of mutations. *Nature Methods* 2018 15:10 15, 816–822.
1863 <https://doi.org/10.1038/s41592-018-0138-4>

1864 Rives, A., Meier, J., Sercu, T., Goyal, S., Lin, Z., Liu, J., Guo, D., Ott, M., Zitnick, C.L., Ma,
1865 J., Fergus, R., 2021. Biological structure and function emerge from scaling unsupervised
1866 learning to 250 million protein sequences. *Proc Natl Acad Sci U S A* 118, e2016239118.
1867 https://doi.org/10.1073/PNAS.2016239118/SUPPL_FILE/PNAS.2016239118.SAPP.PDF
1868 F

1869 Robinson, S.L., Smith, M.D., Richman, J.E., Aukema, K.G., Wackett, L.P., 2020. Machine
1870 learning-based prediction of activity and substrate specificity for OleA enzymes in the
1871 thiolase superfamily. *Synth Biol* 5. <https://doi.org/10.1093/SYNBIO/YSAA004>

1872 Romero-Rivera, A., Corbella, M., Parracino, A., Patrick, W.M., Kamerlin, S.C.L., 2022.
1873 Complex Loop Dynamics Underpin Activity, Specificity, and Evolvability in the ($\beta\alpha$)₈

1874 Barrel Enzymes of Histidine and Tryptophan Biosynthesis. *JACS Au* 2, 943–960.
1875 <https://doi.org/10.1021/jacsau.2c00063>

1876 Romero-Rivera, A., Garcia-Borràs, M., Osuna, S., 2017. Role of Conformational Dynamics
1877 in the Evolution of Retro-Aldolase Activity. *ACS Catal* 7, 8524–8532.
1878 <https://doi.org/10.1021/acscatal.7b02954>

1879 Röttig, M., Rausch, C., Kohlbacher, O., 2010. Combining Structure and Sequence
1880 Information Allows Automated Prediction of Substrate Specificities within Enzyme
1881 Families. *PLoS Comput Biol* 6, e1000636.
1882 <https://doi.org/10.1371/JOURNAL.PCBI.1000636>

1883 Ruiz-Blanco, Y.B., Paz, W., Green, J., Marrero-Ponce, Y., 2015. ProtDCal: A program to
1884 compute general-purpose-numerical descriptors for sequences and 3D-structures of
1885 proteins. *BMC Bioinformatics* 16, 1–15. [https://doi.org/10.1186/S12859-015-0586-](https://doi.org/10.1186/S12859-015-0586-0/TABLES/4)
1886 [0/TABLES/4](https://doi.org/10.1186/S12859-015-0586-0/TABLES/4)

1887 Saito, Y., Oikawa, M., Sato, T., Nakazawa, H., Ito, T., Kameda, T., Tsuda, K., Umetsu, M.,
1888 2021. Machine-Learning-Guided Library Design Cycle for Directed Evolution of
1889 Enzymes: The Effects of Training Data Composition on Sequence Space Exploration.
1890 *ACS Catal* 11, 14615–14624.
1891 https://doi.org/10.1021/ACSCATAL.1C03753/SUPPL_FILE/CS1C03753_SI_007.XLS
1892 X

1893 Sala, D., Engelberger, F., Mchaourab, H.S., Meiler, J., 2023. Modeling conformational states
1894 of proteins with AlphaFold. *Curr Opin Struct Biol* 81, 102645.
1895 <https://doi.org/10.1016/j.sbi.2023.102645>

1896 Sandberg, M., Eriksson, L., Jonsson, J., Sjöström, M., Wold, S., 1998. New chemical
1897 descriptors relevant for the design of biologically active peptides. A multivariate
1898 characterization of 87 amino acids. *J Med Chem* 41, 2481–2491.
1899 https://doi.org/10.1021/JM9700575/SUPPL_FILE/JM2481.PDF

1900 Sanner, M., Olson, A., Spehner, J., 1996. Reduced surface: an efficient way to compute
1901 molecular surfaces. *Biopolymers*. [https://doi.org/10.1002/\(SICI\)1097-0282\(199603\)38:3](https://doi.org/10.1002/(SICI)1097-0282(199603)38:3)
1902 Santacoloma, P.A., Sin, G., Gernaey, K. V., Woodley, J.M., 2011. Multienzyme-catalyzed
1903 processes: Next-generation biocatalysis. *Org Process Res Dev* 15, 203–212.
1904 [https://doi.org/10.1021/OP1002159/ASSET/IMAGES/MEDIUM/OP-2010-](https://doi.org/10.1021/OP1002159/ASSET/IMAGES/MEDIUM/OP-2010-002159_0011.GIF)
1905 [002159_0011.GIF](https://doi.org/10.1021/OP1002159/ASSET/IMAGES/MEDIUM/OP-2010-002159_0011.GIF)

1906 Savile, C.K., Janey, J.M., Mundorff, E.C., Moore, J.C., Tam, S., Jarvis, W.R., Colbeck, J.C.,
1907 Krebber, A., Fleitz, F.J., Brands, J., Devine, P.N., Huisman, G.W., Hughes, G.J., 2010.
1908 Biocatalytic asymmetric synthesis of chiral amines from ketones applied to sitagliptin
1909 manufacture. *Science* (1979) 329, 305–309.
1910 https://doi.org/10.1126/SCIENCE.1188934/SUPPL_FILE/SAVILE.SOM.PDF

1911 Schenkmyerova, A., Pinto, G.P., Toul, M., Marek, M., Hernychova, L., Planas-Iglesias, J.,
1912 Daniel Liskova, V., Pluskal, D., Vasina, M., Emond, S., Dörr, M., Chaloupkova, R.,
1913 Bednar, D., Prokop, Z., Hollfelder, F., Bornscheuer, U.T., Damborsky, J., 2021.
1914 Engineering the protein dynamics of an ancestral luciferase. *Nature Communications*
1915 2021 12:1 12, 1–16. <https://doi.org/10.1038/s41467-021-23450-z>

1916 Schultze, S., Grubmüller, H., 2021. Time-Lagged Independent Component Analysis of
1917 Random Walks and Protein Dynamics. *J. Chem. Theory Comput.* 17, 5766–5776.
1918 <https://doi.org/10.1021/acs.jctc.1c00273>

1919 Schweke, H., Mucchielli, M.H., Chevrollier, N., Gosset, S., Lopes, A., 2022. SURFMAP: A
1920 Software for Mapping in Two Dimensions Protein Surface Features. *J Chem Inf Model*
1921 62, 1595–1601.
1922 https://doi.org/10.1021/ACS.JCIM.1C01269/ASSET/IMAGES/LARGE/CI1C01269_00
1923 [04.JPEG](https://doi.org/10.1021/ACS.JCIM.1C01269/ASSET/IMAGES/LARGE/CI1C01269_00)

1924 Sevgen, E., Moller, J., Lange, A., Parker, J., Quigley, S., Mayer, J., Srivastava, P., Gayatri,
1925 S., Hosfield, D., Korshunova, M., others, 2023. ProT-VAE: Protein Transformer
1926 Variational AutoEncoder for Functional Protein Design. *bioRxiv* 2021–2023.
1927 Sheldon, R.A., Woodley, J.M., 2018. Role of Biocatalysis in Sustainable Chemistry. *Chem*
1928 *Rev* 118, 801–838.
1929 [https://doi.org/10.1021/ACS.CHEMREV.7B00203/ASSET/IMAGES/LARGE/CR-](https://doi.org/10.1021/ACS.CHEMREV.7B00203/ASSET/IMAGES/LARGE/CR-2017-002034_0025.JPEG)
1930 [2017-002034_0025.JPEG](https://doi.org/10.1021/ACS.CHEMREV.7B00203/ASSET/IMAGES/LARGE/CR-2017-002034_0025.JPEG)
1931 Shroff, R., Cole, A.W., Diaz, D.J., Morrow, B.R., Donnell, I., Annapareddy, A., Gollihar, J.,
1932 Ellington, A.D., Thyer, R., 2020. Discovery of novel gain-of-function mutations guided
1933 by structure-based deep learning. *ACS Synth Biol* 9, 2927–2935.
1934 [https://doi.org/10.1021/ACSSYNBIO.0C00345/ASSET/IMAGES/LARGE/SB0C00345](https://doi.org/10.1021/ACSSYNBIO.0C00345/ASSET/IMAGES/LARGE/SB0C00345_0003.JPEG)
1935 [_0003.JPEG](https://doi.org/10.1021/ACSSYNBIO.0C00345/ASSET/IMAGES/LARGE/SB0C00345_0003.JPEG)
1936 Sinai, S., Kelsic, E.D., 2020. A primer on model-guided exploration of fitness landscapes for
1937 biological sequence design. *arXiv preprint arXiv:2010.10614*.
1938 Sledzieski, S., Devkota, K., Singh, R., Cowen, L., Berger, B., 2023. TT3D: Leveraging
1939 precomputed protein 3D sequence models to predict protein–protein interactions.
1940 *Bioinformatics* 39. <https://doi.org/10.1093/BIOINFORMATICS/BTAD663>
1941 Somnath, V.R., Bunne, C., Krause, A., 2021. Multi-Scale Representation Learning on
1942 Proteins. *Adv Neural Inf Process Syst* 34, 25244–25255.
1943 Song, J., Tan, H., Takemoto, K., Akutsu, T., 2008. HSEpred: predict half-sphere exposure
1944 from protein sequences. *Bioinformatics* 24, 1489–1497.
1945 <https://doi.org/10.1093/BIOINFORMATICS/BTN222>
1946 Sperl, J.M., Sieber, V., 2018. Multienzyme Cascade Reactions - Status and Recent Advances.
1947 *ACS Catal* 8, 2385–2396.
1948 [https://doi.org/10.1021/ACSCATAL.7B03440/ASSET/IMAGES/MEDIUM/CS-2017-](https://doi.org/10.1021/ACSCATAL.7B03440/ASSET/IMAGES/MEDIUM/CS-2017-03440Y_0021.GIF)
1949 [03440Y_0021.GIF](https://doi.org/10.1021/ACSCATAL.7B03440/ASSET/IMAGES/MEDIUM/CS-2017-03440Y_0021.GIF)
1950 Steinegger, M., Söding, J., 2017. MMseqs2 enables sensitive protein sequence searching for
1951 the analysis of massive data sets. *Nature Biotechnology* 2017 35:11 35, 1026–1028.
1952 <https://doi.org/10.1038/nbt.3988>
1953 Stimple, S.D., Smith, M.D., Tessier, P.M., 2020. Directed evolution methods for overcoming
1954 trade-offs between protein activity and stability. *AIChE J* 66.
1955 <https://doi.org/10.1002/AIC.16814>
1956 St-Jacques, A.D., Rodriguez, J.M., Eason, M.G., Foster, S.M., Khan, S.T., Damry, A.M.,
1957 Goto, N.K., Thompson, M.C., Chica, R.A., 2023. Computational remodeling of an
1958 enzyme conformational landscape for altered substrate selectivity. *Nat Commun* 14.
1959 <https://doi.org/10.1038/s41467-023-41762-0>
1960 Su, J., Han, C., Zhou, Y., Shan, J., Zhou, X., Yuan, F., 2023. SaProt: Protein Language
1961 Modeling with Structure-aware Vocabulary. *bioRxiv* 2023.10.01.560349.
1962 <https://doi.org/10.1101/2023.10.01.560349>
1963 Taujale, R., Venkat, A., Huang, L.C., Zhou, Z., Yeung, W., Rasheed, K.M., Li, S., Edison,
1964 A.S., Moremen, K.W., Kannan, N., 2020. Deep evolutionary analysis reveals the design
1965 principles of fold a glycosyltransferases. *Elife* 9. <https://doi.org/10.7554/ELIFE.54532>
1966 Teng, S., Srivastava, A.K., Wang, L., 2010. Sequence feature-based prediction of protein
1967 stability changes upon amino acid substitutions. *BMC Genomics* 11, 1–8.
1968 <https://doi.org/10.1186/1471-2164-11-S2-S5/FIGURES/4>
1969 Theodoridis, S., Koutroumbas, K., 2008. Pattern Recognition, Fourth Edition. *Pattern*
1970 *Recognition, Fourth Edition* 1–961. [https://doi.org/10.1016/B978-1-59749-272-](https://doi.org/10.1016/B978-1-59749-272-0.X0001-2)
1971 [0.X0001-2](https://doi.org/10.1016/B978-1-59749-272-0.X0001-2)

- 1972 Thumuluri, V., Almagro Armenteros, J.J., Johansen, A.R., Nielsen, H., Winther, O., 2022.
 1973 DeepLoc 2.0: multi-label subcellular localization prediction using protein language
 1974 models. *Nucleic Acids Res* 50, W228–W234.
- 1975 Tian, J., Dong, X., Wu, T., Wen, P., Liu, X., Zhang, M., An, X., Shi, D., 2024. Revealing the
 1976 conformational dynamics of UDP-GlcNAc recognition by O-GlcNAc transferase via
 1977 Markov state model. *Int J Biol Macromol* 256, 128405.
 1978 <https://doi.org/10.1016/j.ijbiomac.2023.128405>
- 1979 Tokuriki, N., Jackson, C.J., Afriat-Jurnou, L., Wyganowski, K.T., Tang, R., Tawfik, D.S.,
 1980 2012. Diminishing returns and tradeoffs constrain the laboratory optimization of an
 1981 enzyme. *Nature Communications* 2012 3:1 3, 1–10.
 1982 <https://doi.org/10.1038/ncomms2246>
- 1983 Torng, W., Altman, R.B., 2017. 3D deep convolutional neural networks for amino acid
 1984 environment similarity analysis. *BMC Bioinformatics* 18, 1–23.
 1985 <https://doi.org/10.1186/S12859-017-1702-0/FIGURES/8>
- 1986 Trott, O., Olson, A.J., 2010. AutoDock Vina: Improving the speed and accuracy of docking
 1987 with a new scoring function, efficient optimization, and multithreading. *J Comput Chem*
 1988 31, 455–461. <https://doi.org/10.1002/JCC.21334>
- 1989 Tschannen, M., Bachem, O., Lucic, M., 2018. Recent advances in autoencoder-based
 1990 representation learning. arXiv preprint arXiv:1812.05069.
- 1991 Turner, N.J., 2009. Directed evolution drives the next generation of biocatalysts. *Nature*
 1992 *Chemical Biology* 2009 5:8 5, 567–573. <https://doi.org/10.1038/nchembio.203>
- 1993 van Kempen, M., Kim, S.S., Tumescheit, C., Mirdita, M., Lee, J., Gilchrist, C.L.M., Söding,
 1994 J., Steinegger, M., 2023. Fast and accurate protein structure search with Foldseek.
 1995 *Nature Biotechnology* 2023 42:2 42, 243–246. <https://doi.org/10.1038/s41587-023-01773-0>
- 1997 Vani, B.P., Aranganathan, A., Wang, D., Tiwary, P., 2023. AlphaFold2-RAVE: From
 1998 Sequence to Boltzmann Ranking. *J. Chem. Theory Comput.* 19, 4351–4354.
 1999 <https://doi.org/10.1021/acs.jctc.3c00290>
- 2000 Vasina, M., Vanacek, P., Hon, J., Kovar, D., Faldynova, H., Kunka, A., Buryška, T.,
 2001 Badenhorst, C.P.S., Mazurenko, S., Bednar, D., Stavrakis, S., Bornscheuer, U.T.,
 2002 deMello, A., Damborsky, J., Prokop, Z., 2022. Advanced database mining of efficient
 2003 haloalkane dehalogenases by sequence and structure bioinformatics and microfluidics.
 2004 *Chem Catalysis* 2, 2704–2725. <https://doi.org/10.1016/J.CHECAT.2022.09.011>
- 2005 Vaswani, A., Shazeer, N., Parmar, N., Uszkoreit, J., Jones, L., Gomez, A.N., Kaiser, Ł.,
 2006 Polosukhin, I., 2017. Attention is all you need. *Adv Neural Inf Process Syst* 30.
- 2007 Verkuil, R., Kabeli, O., Du, Y., Wicky, B.I.M., Milles, L.F., Dauparas, J., Baker, D.,
 2008 Ovchinnikov, S., Sercu, T., Rives, A., 2022. Language models generalize beyond natural
 2009 proteins. *bioRxiv* 2012–2022.
- 2010 Vilone, G., Longo, L., 2020. Explainable Artificial Intelligence: a Systematic Review.
- 2011 Vincent, P., Larochelle, H., Bengio, Y., Manzagol, P.-A., 2008. Extracting and composing
 2012 robust features with denoising autoencoders, in: *Proceedings of the 25th International*
 2013 *Conference on Machine Learning*. pp. 1096–1103.
- 2014 Waksman, T., Astin, E., Fisher, S.R., Hunter, W., Bos, J., 2024. Computational prediction of
 2015 structure, function and interaction of *Myzus persicae* (green peach aphid) salivary
 2016 effector proteins. *Mol Plant Microbe Interact.* <https://doi.org/10.1094/MPMI-10-23-0154-FI>
- 2017
- 2018 Wallach, I., Heifets, A., 2018. Most Ligand-Based Classification Benchmarks Reward
 2019 Memorization Rather than Generalization. *J Chem Inf Model* 58, 916–932.
 2020 https://doi.org/10.1021/ACS.JCIM.7B00403/SUPPL_FILE/CI7B00403_SI_002.PDF

- 2021 Wang, K., Zhou, R., Tang, J., Li, M., 2023. GraphscoreDTA: optimized graph neural network
2022 for protein–ligand binding affinity prediction. *Bioinformatics* 39.
2023 <https://doi.org/10.1093/BIOINFORMATICS/BTAD340>
- 2024 Wang, Y., Wei, Z., Xi, L., 2022. Sfenn: a novel scoring function based on 3D convolutional
2025 neural network for accurate and stable protein–ligand affinity prediction. *BMC*
2026 *Bioinformatics* 23, 1–18. <https://doi.org/10.1186/S12859-022-04762-3/FIGURES/5>
- 2027 Wapeesittipan, P., Mey, A.S.J.S., Walkinshaw, M.D., Michel, J., 2019. Allosteric effects in
2028 cyclophilin mutants may be explained by changes in nano-microsecond time scale
2029 motions. *Commun Chem* 2, 1–9. <https://doi.org/10.1038/s42004-019-0136-1>
- 2030 Wayment-Steele, H.K., Ojoawo, A., Otten, R., Aplitz, J.M., Pitsawong, W., Hömberger, M.,
2031 Ovchinnikov, S., Colwell, L., Kern, D., 2024. Predicting multiple conformations via
2032 sequence clustering and AlphaFold2. *Nature* 625, 832–839.
2033 <https://doi.org/10.1038/s41586-023-06832-9>
- 2034 Weinert, T., Olieric, N., Cheng, R., Brünle, S., James, D., Ozerov, D., Gashi, D., Vera, L.,
2035 Marsh, M., Jaeger, K., Dworkowski, F., Panepucci, E., Basu, S., Skopintsev, P., Doré,
2036 A.S., Geng, T., Cooke, R.M., Liang, M., Prota, A.E., Panneels, V., Nogly, P., Ermler,
2037 U., Schertler, G., Hennig, M., Steinmetz, M.O., Wang, M., Standfuss, J., 2017. Serial
2038 millisecond crystallography for routine room-temperature structure determination at
2039 synchrotrons. *Nat Commun* 8, 542. <https://doi.org/10.1038/s41467-017-00630-4>
- 2040 Wellawatte, G.P., Gandhi, H.A., Seshadri, A., White, A.D., 2023. A Perspective on
2041 Explanations of Molecular Prediction Models. *J Chem Theory Comput* 19, 2149–2160.
2042 https://doi.org/10.1021/ACS.JCTC.2C01235/ASSET/IMAGES/LARGE/CT2C01235_0
2043 005.JPEG
- 2044 Witek, J., Smusz, S., Rataj, K., Mordalski, S., Bojarski, A.J., 2014. An application of
2045 machine learning methods to structural interaction fingerprints—a case study of kinase
2046 inhibitors. *Bioorg Med Chem Lett* 24, 580–585.
2047 <https://doi.org/10.1016/j.bmcl.2013.12.017>
- 2048 Wittmann, Bruce J, Johnston, K.E., Wu, Z., Arnold, F.H., 2021. Advances in machine
2049 learning for directed evolution. *Curr Opin Struct Biol* 69, 11–18.
- 2050 Wittmann, Bruce J., Yue, Y., Arnold, F.H., 2021. Informed training set design enables
2051 efficient machine learning-assisted directed protein evolution. *Cell Syst* 12, 1026-
2052 1045.e7. <https://doi.org/10.1016/J.CELS.2021.07.008>
- 2053 Wojciech Samek, Grégoire Montavon, Andrea Vedaldi, Lars Kai Hansen, Klaus-Robert
2054 Müller, 2019. Explainable AI: Interpreting, Explaining and Visualizing Deep Learning,
2055 Lecture Notes in Computer Science. Springer International Publishing, Cham.
2056 <https://doi.org/10.1007/978-3-030-28954-6>
- 2057 Wold, S., Eriksson, L., Hellberg, S., Jonsson, J., Sjostrom, M., Skagerberg, B., Wikstrom, C.,
2058 2011. Principal property values for six non-natural amino acids and their application to a
2059 structure–activity relationship for oxytocin peptide analogues.
2060 <https://doi.org/10.1139/v87-305> 65, 1814–1820. <https://doi.org/10.1139/V87-305>
- 2061 Wolf-Watz, M., Thai, V., Henzler-Wildman, K., Hadjipavlou, G., Eisenmesser, E.Z., Kern,
2062 D., 2004. Linkage between dynamics and catalysis in a thermophilic-mesophilic enzyme
2063 pair. *Nat Struct Mol Biol* 11, 945–949. <https://doi.org/10.1038/nsmb821>
- 2064 Woodley, J.M., 2022. Ensuring the Sustainability of Biocatalysis. *ChemSusChem* 15,
2065 e202102683. <https://doi.org/10.1002/CSSC.202102683>
- 2066 Wu, S., Snajdrova, R., Moore, J.C., Baldenius, K., Bornscheuer, U.T., 2021. Biocatalysis:
2067 Enzymatic Synthesis for Industrial Applications. *Angewandte Chemie International*
2068 *Edition* 60, 88–119. <https://doi.org/10.1002/ANIE.202006648>
- 2069 Wu, Z., Jennifer Kan, S.B., Lewis, R.D., Wittmann, B.J., Arnold, F.H., 2019. Machine
2070 learning-assisted directed protein evolution with combinatorial libraries. *Proc Natl Acad*

2071 Sci U S A 116, 8852–8858.
2072 https://doi.org/10.1073/PNAS.1901979116/SUPPL_FILE/PNAS.1901979116.SAPP.PD
2073 F
2074 Xia, C., Feng, S.H., Xia, Y., Pan, X., Shen, H. Bin, 2023. Leveraging scaffold information to
2075 predict protein-ligand binding affinity with an empirical graph neural network. *Brief*
2076 *Bioinform* 24. <https://doi.org/10.1093/BIB/BBAC603>
2077 Xiao, S., Tian, H., Tao, P., 2022. PASSer2.0: Accurate Prediction of Protein Allosteric Sites
2078 Through Automated Machine Learning. *Front Mol Biosci* 9, 879251.
2079 <https://doi.org/10.3389/FMOLB.2022.879251/BIBTEX>
2080 Xu, G., Dou, Z., Chen, Xuanzao, Zhu, L., Zheng, X., Chen, Xiaoyu, Xue, J., Niwayama, S.,
2081 Ni, Y., 2024. Enhanced stereodivergent evolution of carboxylesterase for efficient
2082 kinetic resolution of near-symmetric esters through machine learning.
2083 <https://doi.org/10.21203/RS.3.RS-3897762/V1>
2084 Xu, Y., Verma, D., Sheridan, R.P., Liaw, A., Ma, J., Marshall, N.M., McIntosh, J., Sherer,
2085 E.C., Svetnik, V., Johnston, J.M., 2020. Deep Dive into Machine Learning Models for
2086 Protein Engineering. *J Chem Inf Model* 60, 2773–2790.
2087 https://doi.org/10.1021/ACS.JCIM.0C00073/ASSET/IMAGES/LARGE/CI0C00073_00
2088 08.JPEG
2089 Xu, Z., Wu, J., Song, Y.S., Mahadevan, R., 2022. Enzyme Activity Prediction of Sequence
2090 Variants on Novel Substrates using Improved Substrate Encodings and Convolutional
2091 Pooling.
2092 Yamada, H., Kobayashi, M., 1996. Nitrile hydratase and its application to industrial
2093 production of acrylamide. *Biosci Biotechnol Biochem* 60, 1391–1400.
2094 <https://doi.org/10.1271/BBB.60.1391>
2095 Yang, J., Li, F.-Z., Arnold, F.H., 2024. Opportunities and Challenges for Machine Learning-
2096 Assisted Enzyme Engineering. *ACS Cent Sci*.
2097 <https://doi.org/10.1021/ACSCENTSCI.3C01275>
2098 Yang, K.K., Eleutherai, N.Z., Yeh, H., 2022. Masked inverse folding with sequence transfer
2099 for protein representation learning. *bioRxiv* 2022.05.25.493516.
2100 <https://doi.org/10.1101/2022.05.25.493516>
2101 Yang, K.K., Wu, Z., Arnold, F.H., 2019. Machine-learning-guided directed evolution for
2102 protein engineering. *Nature Methods* 2019 16:8 16, 687–694.
2103 <https://doi.org/10.1038/s41592-019-0496-6>
2104 Yang, L., Yang, G., Chen, X., Yang, Q., Yao, X., Bing, Z., Niu, Y., Huang, L., Yang, Lei,
2105 2021. Deep Scoring Neural Network Replacing the Scoring Function Components to
2106 Improve the Performance of Structure-Based Molecular Docking. *ACS Chem Neurosci*
2107 12, 2133–2142.
2108 https://doi.org/10.1021/ACSCHEMNEURO.1C00110/SUPPL_FILE/CN1C00110_SI_0
2109 01.PDF
2110 Yang, M., Fehl, C., Lees, K. V., Lim, E.K., Offen, W.A., Davies, G.J., Bowles, D.J.,
2111 Davidson, M.G., Roberts, S.J., Davis, B.G., 2018. Functional and informatics analysis
2112 enables glycosyltransferase activity prediction. *Nat Chem Biol* 14, 1109–1117.
2113 <https://doi.org/10.1038/S41589-018-0154-9>
2114 Yang, Y., Gao, J., Wang, J., Heffernan, R., Hanson, J., Paliwal, K., Zhou, Y., 2018. Sixty-
2115 five years of the long march in protein secondary structure prediction: the final stretch?
2116 *Brief Bioinform* 19, 482–494. <https://doi.org/10.1093/BIB/BBW129>
2117 Yang, Y., Niroula, A., Shen, B., Vihinen, M., 2016. PON-Sol: prediction of effects of amino
2118 acid substitutions on protein solubility. *Bioinformatics* 32, 2032–2034.
2119 <https://doi.org/10.1093/BIOINFORMATICS/BTW066>

2120 Yang, Y., Zeng, L., Vihinen, M., 2021. PON-Sol2: Prediction of Effects of Variants on
2121 Protein Solubility. *Int J Mol Sci* 22. <https://doi.org/10.3390/IJMS22158027>

2122 Yang, Z., Zhong, W., Lv, Q., Dong, T., Yu-Chian Chen, C., 2023. Geometric Interaction
2123 Graph Neural Network for Predicting Protein-Ligand Binding Affinities from 3D
2124 Structures (GIGN). *Journal of Physical Chemistry Letters* 14, 2020–2033.
2125 https://doi.org/10.1021/ACS.JPCLETT.2C03906/SUPPL_FILE/JZ2C03906_SI_001.PDF
2126 F

2127 Yang, Z., Zhong, W., Zhao, L., Yu-Chian Chen, C., 2022. MGraphDTA: deep multiscale
2128 graph neural network for explainable drug–target binding affinity prediction. *Chem Sci*
2129 13, 816–833. <https://doi.org/10.1039/D1SC05180F>

2130 Yeh, A.H.W., Norn, C., Kipnis, Y., Tischer, D., Pellock, S.J., Evans, D., Ma, P., Lee, G.R.,
2131 Zhang, J.Z., Anishchenko, I., Coventry, B., Cao, L., Dauparas, J., Halabiya, S., DeWitt,
2132 M., Carter, L., Houk, K.N., Baker, D., 2023. De novo design of luciferases using deep
2133 learning. *Nature* 2023 614:7949 614, 774–780. [https://doi.org/10.1038/s41586-023-](https://doi.org/10.1038/s41586-023-05696-3)
2134 05696-3

2135 Yosinski, J., Clune, J., Bengio, Y., Lipson, H., 2014. How transferable are features in deep
2136 neural networks? *Adv Neural Inf Process Syst* 27.

2137 Yu, T., Cui, H., Li, J.C., Luo, Y., Jiang, G., Zhao, H., 2023. Enzyme function prediction
2138 using contrastive learning. *Science* (1979) 379, 1358–1363.

2139 Zaretzki, J., Bergeron, C., Rydberg, P., Huang, T.W., Bennett, K.P., Breneman, C.M., 2011.
2140 RS-predictor: A new tool for predicting sites of cytochrome P450-mediated metabolism
2141 applied to CYP 3A4. *J Chem Inf Model* 51, 1667–1689.
2142 https://doi.org/10.1021/CI2000488/SUPPL_FILE/CI2000488_SI_001.ZIP

2143 Zaretzki, J., Matlock, M., Swamidass, S.J., 2013. XenoSite: Accurately predicting cyp-
2144 mediated sites of metabolism with neural networks. *J Chem Inf Model* 53, 3373–3383.
2145 https://doi.org/10.1021/CI400518G/SUPPL_FILE/CI400518G_SI_002.ZIP

2146 Zhao, H., Arnold, F.H., 1999. Directed evolution converts subtilisin E into a functional
2147 equivalent of thermitase. *Protein Engineering, Design and Selection* 12, 47–53.
2148 <https://doi.org/10.1093/PROTEIN/12.1.47>

2149 Zhou, J., Cui, G., Hu, S., Zhang, Z., Yang, C., Liu, Z., Wang, L., Li, C., Sun, M., 2020.
2150 Graph neural networks: A review of methods and applications. *AI Open* 1, 57–81.
2151 <https://doi.org/10.1016/J.AIOPEN.2021.01.001>

2152 Zhou, J., Troyanskaya, O.G., 2015. Predicting effects of noncoding variants with deep
2153 learning–based sequence model. *Nature Methods* 2015 12:10 12, 931–934.
2154 <https://doi.org/10.1038/nmeth.3547>
2155